Mutations in *Escherichia coli* Polyphosphate Kinase That Lead to Dramatically Increased *In Vivo* Polyphosphate Levels

Amanda K. Rudat,[a] Arya Pokhrel,[a] Todd J. Green,[a] Michael J. Gray[a]

[a]Department of Microbiology, School of Medicine, University of Alabama at Birmingham, Birmingham, Alabama, USA

ABSTRACT Bacteria synthesize inorganic polyphosphate (polyP) in response to a wide variety of stresses, and production of polyP is essential for stress response and survival in many important pathogens and bacteria used in biotechnological processes. However, surprisingly little is known about the molecular mechanisms that control polyP synthesis. We have therefore developed a novel genetic screen that specifically links growth of *Escherichia coli* to polyP synthesis, allowing us to isolate mutations leading to enhanced polyP production. Using this system, we have identified mutations in the polyP-synthesizing enzyme polyP kinase (PPK) that lead to dramatic increases in *in vivo* polyP synthesis but do not substantially affect the rate of polyP synthesis by PPK *in vitro*. These mutations are distant from the PPK active site and found in interfaces between monomers of the PPK tetramer. We have also shown that high levels of polyP lead to intracellular magnesium starvation. Our results provide new insights into the control of bacterial polyP accumulation and suggest a simple, novel strategy for engineering bacteria with increased polyP contents.

IMPORTANCE PolyP is an ancient, universally conserved biomolecule and is important for stress response, energy metabolism, and virulence in a remarkably broad range of microorganisms. PolyP accumulation by bacteria is also important in biotechnology applications. For example, it is critical to enhanced biological phosphate removal (EBPR) from wastewater. Understanding how bacteria control polyP synthesis is therefore of broad importance in both the fields of bacterial pathogenesis and biological engineering. Using *Escherichia coli* as a model organism, we have identified the first known mutations in polyP kinase that lead to increases in cellular polyP content.

KEYWORDS inorganic polyphosphate, bacterial genetics, mutagenesis, enzyme engineering, stress response, inorganic polyphosphate

Inorganic polyphosphate (polyP) is an ancient, universally conserved biopolymer composed of linear chains of phosphate residues linked by high-energy phosphoanhydride bonds (1, 2). PolyP ranges from three to hundreds of phosphate units long and plays many roles in cellular physiology. In vertebrates, in which the enzyme(s) of polyP synthesis is not yet known, polyP is involved in processes as diverse as blood clotting, inflammation, bone mineralization, neurotransmission, and amyloid protein aggregation (3–7). In bacteria, in which polyP is synthesized by the polyP kinase (PPK) (8, 9), polyP has been shown to act as a protein-stabilizing chaperone, a regulator of protease activity, a chelator of heavy metals, an energy source, and a phosphate reservoir, and it plays important roles in a variety of stress responses, DNA damage repair, the cell cycle, motility, and biofilm formation (1, 10–21). Notably, loss of the PPK-encoding *ppk* gene causes a wide variety of bacterial pathogens to become avirulent (e.g., see references 22 to 28), so an improved understanding of bacterial polyP metabolism could have profound implications for the control of infectious diseases. From a bio-

technology perspective, bacterial polyP accumulation not only is interesting as a method of increasing the stress tolerance of bacteria (1, 19) or as an energy source to drive enzymatic reactions (16) but also is a critical component of wastewater treatment (enhanced biological phosphate removal [EBPR]) (29–31). However, previous attempts to engineer bacteria to produce increased amounts of polyP have been only moderately successful (32–35).

Given the importance of polyP in bacterial physiology, it is surprising how little is known about how bacteria regulate polyP synthesis. This issue was last addressed by the late Nobel laureate Arthur Kornberg, who discovered all of the known bacterial enzymes of polyP metabolism (8, 9, 36, 37). In work published 20 years ago, his lab identified several genes involved in controlling stress-induced polyP accumulation in *Escherichia coli* but did not establish the mechanism(s) by which most of them act (38, 39). It has been reported that during some kinds of starvation stress, the small molecule alarmone (p)ppGpp (40, 41) is required for polyP accumulation (38, 42), at least partly due to its ability to inhibit the polyP-degrading exopolyphosphatase (PPX) (39). PolyP accumulation after other stresses has been reported to not necessarily depend on (p)ppGpp, but it may require other genes, including those encoding the phosphate starvation-responsive transcription factor PhoB, the nitrogen starvation-responsive transcription factor NtrC, and the general stress response sigma factor RpoS (38, 42). However, neither PhoB nor NtrC regulates transcription of the *ppk-ppx* operon in *E. coli* (43–45), and while there is one report that transcription of *ppk* is controlled by RpoS (46), multiple other studies have found no such regulation (47–53). PolyP is itself necessary for efficient transcription of *rpoS* (54–56), complicating the issue even further. More recent work has shown that mutants lacking PhoU, an inhibitor of phosphate uptake (57), constitutively accumulate polyP (58, 59), but this has done little to clarify the molecular mechanisms by which polyP synthesis is controlled.

In this work, we have demonstrated that PPX is not required for induction of polyP synthesis by nutrient limitation stress in *E. coli* and have developed a novel genetic tool that allows us to isolate mutants specifically modified in polyP synthesis. We have used this tool to isolate point mutants of *ppk* which accumulate extraordinarily high levels of polyP both in the absence and presence of stress *in vivo*. These mutations are found on the surface regions of PPK monomers, are not near the active site, and do not appear to encode enzymes with enhanced polyP synthase activity *in vitro*, suggesting that they affect a previously unknown *in vivo* regulatory interaction.

RESULTS

Regulation of polyP accumulation is not solely dependent on modulation of PPX activity. PPX is allosterically inhibited by (p)ppGpp during amino acid starvation (39) and is oxidatively inactivated by hypochlorous acid (HOCl) (14), two stresses which lead to substantial polyP accumulation. Based on this and the fact that polyP and (p)ppGpp levels rise concurrently during stress in many bacterial species (42, 60–62), most models of bacterial polyP regulation in the literature focus on PPX inhibition as a key factor in controlling polyP accumulation (39, 60, 63, 64), although this is known to be an oversimplification (38). We observed that a mutant that lacks PPX does not produce constitutively high levels of polyP and was still able to induce polyP synthesis in response to nutrient limitation in this case, a shift from exponential growth in lysogeny broth (LB) medium, during which *E. coli* contains no detectable polyP (38), into morpholinopropanesulfonic acid (MOPS) minimal medium containing no amino acids, 4 g liter^{-1} of glucose, and 0.1 mM K_2HPO_4 (Fig. 1A). The same pattern is seen with HOCl-stressed cells (14). Therefore, the main role of PPX inhibition likely lies in controlling the amount of polyP that accumulates once synthesis is activated. As previously reported, a mutant lacking PPK makes no detectable polyP under any condition, and a mutant lacking the phosphate starvation-inducible transcription factor PhoB accumulates very little polyP after stress (Fig. 1A).

There is some debate in the literature about the best way to measure *in vivo* polyP levels. We used a simple silica column-based extraction method (14, 38, 65) which has
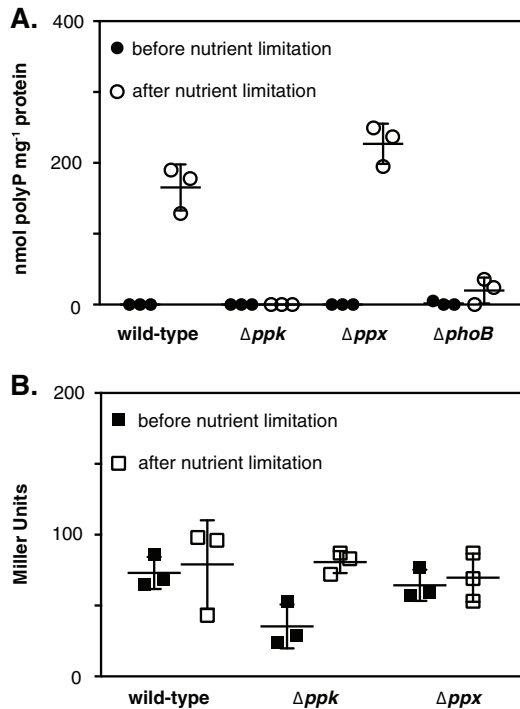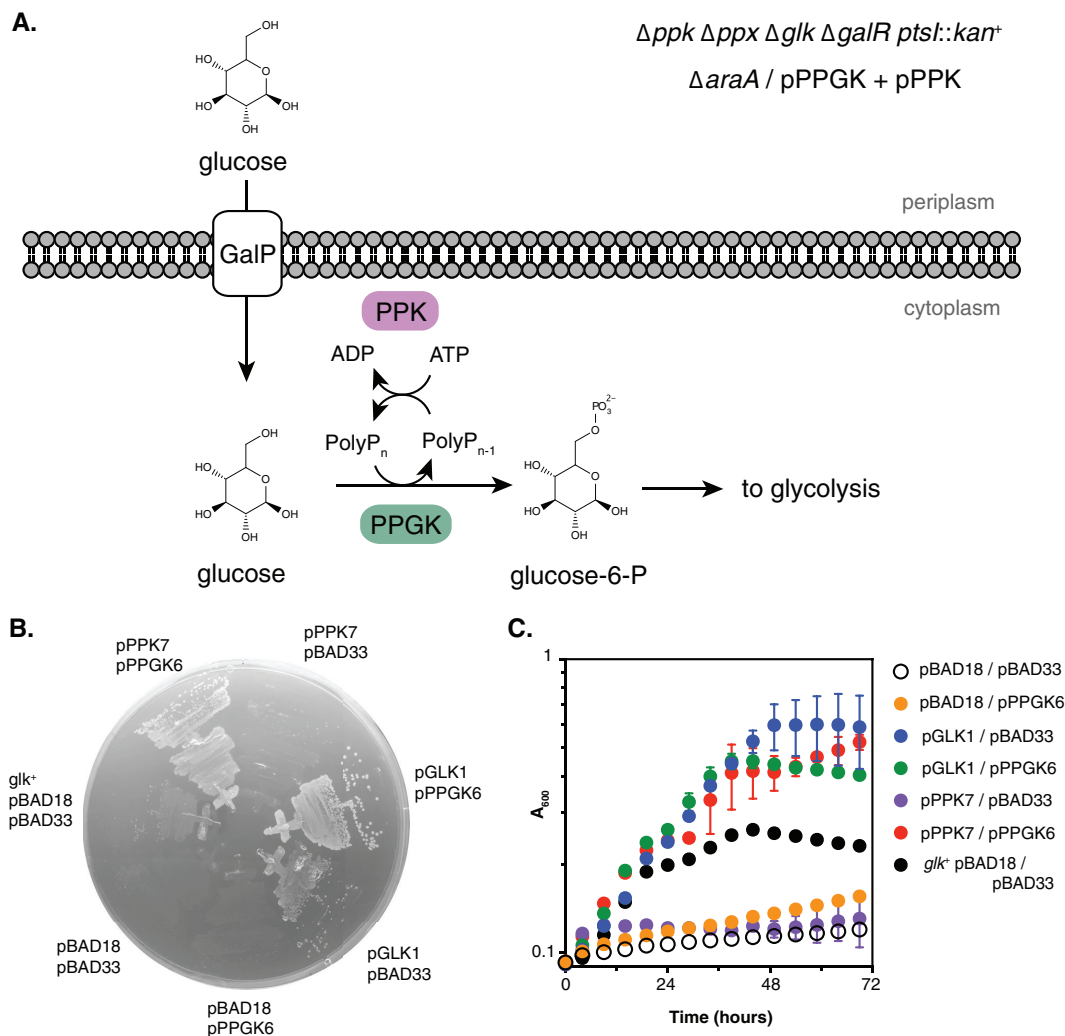
FIG 1 Regulation of polyP synthesis by nutrient limitation stress does not depend on *ppx* or upregulation of *ppk*. (A) *E. coli* MG1655 (wild-type) and isogenic Δ*ppk*, Δ*ppx*, or Δ*phoB* strains were grown at 37°C to an A_{600} of 0.25 to 0.3 in rich medium (LB) and then shifted for 2 h to MOPS minimal medium with no amino acids, 4 g liter^{-1} of glucose, and 0.1 mM K_2HPO_4 (n = 3; means ± SDs). PolyP concentrations are in terms of individual phosphate monomers. (B) *E. coli* MG1655 (wild-type) and isogenic Δ*ppk* and Δ*ppx* strains containing the P$_{ppk}$-*uidA* fusion plasmid pGUSA5 were grown at 37°C to mid-log phase in rich medium (LB) and then shifted for 2 h to MOPS minimal medium with no amino acids, 4 g liter^{-1} of glucose, and 0.1 mM K_2HPO_4 (n = 3; values are means ± SDs). Expression from the P$_{ppk}$ promoter was determined using β-glucuronidase activity assays.

been widely used but does not efficiently extract short-chain polyP (66). We therefore confirmed our results using gel electrophoresis (67, 68) of unextracted cell lysates, a more qualitative method which nevertheless illustrated the presence of high levels of polyP only in *ppk*$^+$ cells after stress, and also showed that there was no substantial difference in the distribution of polyP chain lengths produced by the wild type and Δ*ppx* mutants under nutrient stress conditions (see Fig. S1 in the supplemental material).

The above-described results indicate that the current model explaining how *E. coli* regulates polyP synthesis is incomplete, which is a significant limitation in engineering bacteria with enhanced polyP content. Transcription of the *ppk-ppx* operon did not change in wild-type or Δ*ppx* cells upon either nutrient limitation (Fig. 1B) or HOCl stress (69, 70), although surprisingly, expression was significantly (Student's *t* test, $P < 0.05$) lower in rich medium in Δ*ppk* cells. This might indicate a previously unknown role for PPK or polyP in *ppk* expression, but changes in the expression of *ppk-ppx* could not explain the increase in polyP levels after nutrient limitation. We hypothesized, therefore, that the activity of the PPK enzyme itself might be regulated, and we set about designing a genetic screen to identify amino acids in PPK involved in control of polyP synthesis.

Construction of a polyP synthesis-dependent *E. coli* strain. An *E. coli* mutant lacking *ppk* has defects in multiple stress responses, biofilm formation, virulence, antibiotic resistance, and motility (1, 9, 14, 71), but none of these phenotypes are specific to a lack of polyP. This has hindered the use of genetics in deciphering the regulation of polyP synthesis. To address this long-standing problem and allow isolation of mutants with altered regulation or activity of PPK, we constructed a strain of *E.*

FIG 2 PolyP-dependent growth of *E. coli* strain MJG722 (Δ*araA* Δ*ppk* Δ*ppx* Δ*glk* Δ*galR ptsI::kan*$^+$). (A) Strategy for engineering an *E. coli* strain in which growth on glucose is dependent on high levels of polyP synthesis. Deletion of *glk* and *ptsI* eliminates both natural pathways for glucose phosphorylation in *E. coli* but also eliminates PTS-dependent glucose import. Deletion of *galR* leads to overproduction of the galactose permease GalP, which allows glucose to enter the cell. Expression of the polyP-dependent glucokinase PPGK from a plasmid allows phosphorylation of glucose, and therefore growth on glucose as a sole carbon source, only in the presence of high levels of PPK polyP synthesis activity. Due to deletion of the chromosomal *ppk-ppx* operon, this strain depends on plasmid-encoded PPK for polyP synthesis. Deletion of *araA* prevents arabinose catabolism and allows the use of arabinose-inducible promoters in pPPGK and pPPK plasmids. (B and C) MJG722 and the *glk*$^+$ strain MJG721 (Δ*araA* Δ*ppk* Δ*ppx* Δ*galR ptsI::kan*$^+$), transformed with the indicated plasmids, were incubated on M9 minimal medium containing 0.2% glucose, 0.2% arabinose, and 0.025% Casamino Acids for 2 days at 37°C (B) or grown overnight in LB containing ampicillin and chloramphenicol, rinsed once with PBS, and resuspended to an A_{600} of 0.1 in M9 minimal medium containing 0.2% glucose, 0.2% arabinose, and 0.025% Casamino Acids (C). Cultures were incubated with shaking at 37°C in a Tecan Infinite M1000 plate reader, and A_{600} was measured every 5 h (*n* = 3 or 4; values are means ± SDs).

coli in which growth on glucose was dependent on high levels of polyP biosynthesis (Fig. 2A). We took advantage of the existence of strictly polyP-dependent glucokinase (PPGK) enzymes from cyanobacteria that cannot use nucleoside triphosphates (NTPs) as phosphodonors (16, 17). We codon optimized the gene for one such enzyme, *all1371* (here referred to as *ppgK*), from *Anabaena* sp. strain PCC 7120 (17), for expression in *E. coli* and cloned it into a plasmid with an arabinose-inducible promoter (72). *E. coli* has two glucose phosphorylation systems that catalyze the essential first step in assimilating glucose via glycolysis: the ATP-dependent cytoplasmic enzyme glucokinase (GLK; encoded by the *glk* gene) and the phosphoenolpyruvate-dependent phosphotransferase system (PTS), which phosphorylates glucose during its transport across the cell membrane (73–75). We deleted both systems (76), constructing a strain lacking both *glk*

and the critical PTS gene *ptsI*. *E. coli* strains lacking the PTS are unable to take up glucose efficiently (75), so we also deleted *galR*, the repressor of galactose utilization, a mutation that leads to overproduction of GalP, a permease which can transport glucose into the cell without phosphorylation (77, 78). Combining these mutations with a deletion of the arabinose catabolism gene *araA* (75) and a deletion of the *ppk-ppx* operon (8, 37) yielded strain MJG722 (Δ*araA* Δ*ppk* Δ*ppx* Δ*glk* Δ*galR ptsI::kan*+).

When transformed with empty vector controls, MJG722 did not grow on minimal medium containing glucose and arabinose (Fig. 2B and C). Expression of PPGK alone did not improve growth, although expression of the ATP-dependent *E. coli* GLK permitted robust growth. Overexpression of PPK from high-copy-number plasmids transiently increases polyP levels in *E. coli* in high-phosphate media (32, 34, 35). In the absence of PPGK, expression of PPK from an arabinose-inducible promoter on the high-copy-number plasmid pPPK7 (14) did not improve growth of MJG722 on glucose, indicating that polyP production alone was not sufficient to rescue this strain. However, when both PPK and PPGK were expressed, the cells grew well, indicating that this strain was indeed dependent on polyP-driven glucose phosphorylation for growth on glucose. As a final control, we tested the ability of the *glk*+ strain MJG721 (Δ*araA* Δ*ppk* Δ*ppx* Δ*galR ptsI::kan*+), transformed with empty vectors, to grow on glucose. This strain grew, albeit less well than the equivalent strain expressing *glk* from a plasmid, indicating that glucokinase activity is probably the limiting factor for growth under these conditions. These phenotypes were observed both on solid and in liquid media, indicating that the larger colonies formed by the *ppk*+ *ppgk*+ strain on plates were not the result of differences in inoculation levels.

Isolation of *ppk* mutants leading to enhanced polyP accumulation (*ppk** alleles). Next, we cloned *ppk* and its native promoter into the low-copy-number vector pWSK129 (79). This plasmid (pPPK10), unlike the high-copy-number arabinose-inducible *ppk* plasmid pPPK7, allowed only very poor growth of the restrictive strain MJG870 (Δ*araA* Δ*ppk* Δ*ppx* Δ*glk* Δ*galR* Δ*ptsI*/pPPGK6 [*ppgK*+]) on glucose (Fig. 3A and B), and this strain accumulated no detectable polyP in rich media (Fig. 3D), supporting the hypothesis that wild-type PPK is largely inactive under nonstress conditions.

We randomly mutagenized pPPK10 using the *E. coli* XL1-Red mutator strain (Agilent Technologies) and transformed the resulting pool of plasmids into MJG870, isolating mutants that grew robustly on glucose on both solid and liquid media (Fig. 3A and B; see also Fig. S2). We sequenced 21 such mutants, identifying 9 different mutated *ppk* genes which we refer to here as *ppk** alleles (Table 1). Two of these alleles were double mutants containing one mutation that we isolated independently plus one additional mutation, so we concluded that we had identified 7 amino acid changes in PPK capable of allowing growth under our restrictive conditions. As expected from our use of XL1-Red, most of the mutations isolated were G-to-A transitions (80). We found no promoter mutations, consistent with there being little role for transcription in control of stress-induced polyP accumulation in *E. coli*. The strains containing *ppk** plasmids had substantial growth defects when grown in rich medium (Fig. 3C) (see also below).

To confirm that our mutagenesis strategy was successful at isolating strains with enhanced polyP synthesis, we directly measured polyP levels in MJG870 containing *ppk** mutant plasmids. All seven strains produced very high levels of polyP when grown to mid-log phase in either minimal or rich medium (Fig. 3D), conditions under which cells containing chromosomally or pPPK10-encoded wild-type *ppk* either did not grow or produced no detectable polyP. In contrast, overexpression of wild-type *ppk* from the arabinose-inducible pPPK7 plasmid under these conditions resulted in very large amounts of polyP in minimal medium but no detectable polyP in rich medium, indicating that the effect of *ppk** alleles was not the same as the effect of simply overexpressing wild-type PPK.

***ppk** alleles dramatically enhance *in vivo* polyP accumulation.** To assess the role of *ppk** mutations in a more nearly physiological genetic background, we transformed each *ppk** plasmid into a Δ*ppk* strain of *E. coli* and measured polyP levels before and
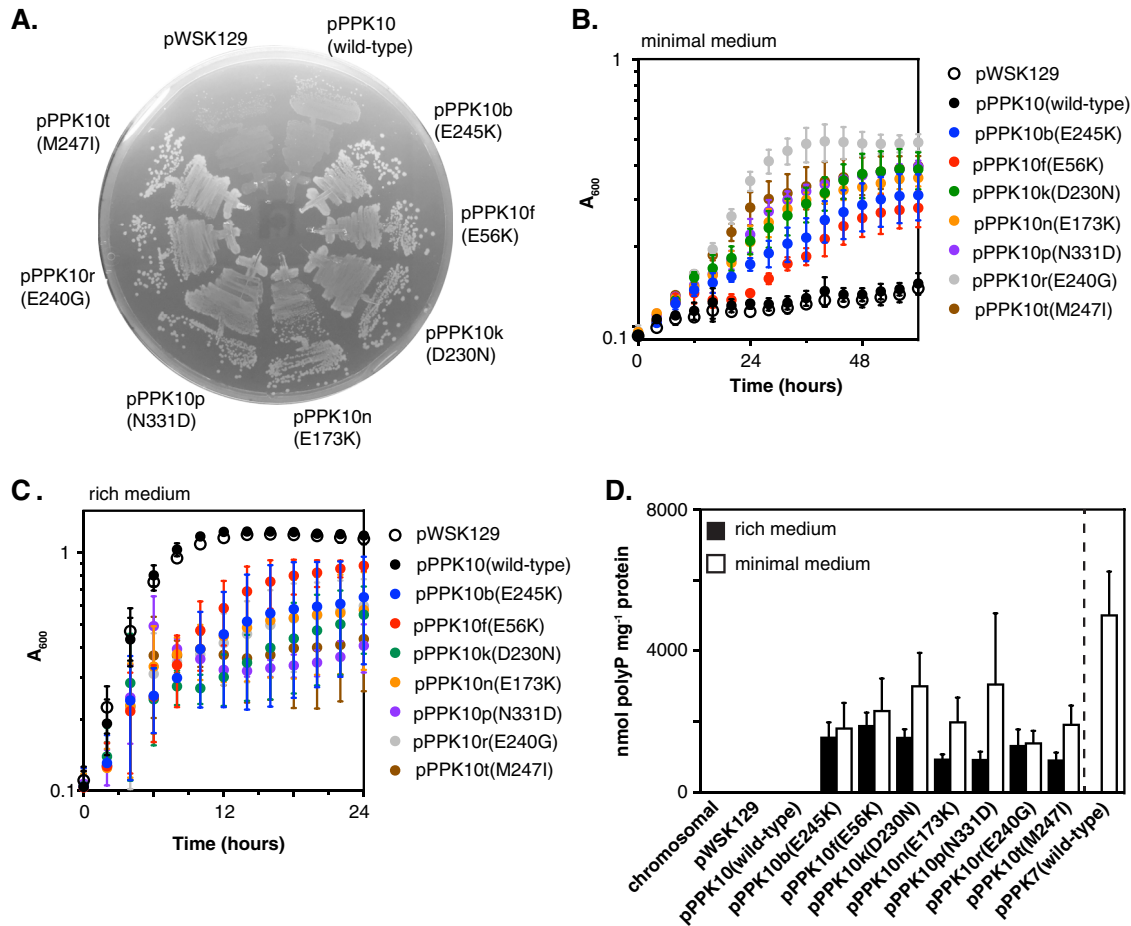
FIG 3 Screen for increased polyP synthesis. (A to C) MJG870 ($\Delta araA$ Δppk Δppx Δglk $\Delta galR$ $\Delta ptsI$/pPPGK6 [$ppgK^+$]) containing mutated ppk^* alleles in pPPK10-derived plasmids was incubated for 2 days at 37°C on M9 minimal medium containing 0.2% glucose, 0.2% arabinose, and 0.025% Casamino Acids (A) or grown overnight in LB containing kanamycin and chloramphenicol, rinsed once with PBS, and resuspended to an A_{600} of 0.1 in M9 minimal medium containing 0.2% glucose, 0.2% arabinose, and 0.025% Casamino Acids (B) or LB containing kanamycin and chloramphenicol (C). Cultures were incubated with shaking at 37°C in a Tecan Infinite M1000 plate reader ($n = 3$ to 6; values are means ± SDs). (D) MJG621 ($\Delta araA$; chromosomal wild type for ppk), MJG870 ($\Delta araA$ Δppk Δppx Δglk $\Delta galR$ $\Delta ptsI$/pPPGK6 [$ppgK^+$]) containing the indicated plasmids, and MJG722 ($\Delta araA$ Δppk Δppx Δglk $\Delta galR$ $ptsI$::kan^+/pPPGK6 [$ppgK^+$]) containing pPPK7 (to the right of the dashed line) were grown to an A_{600} of 0.25 to 0.3 in rich medium (LB), containing kanamycin or ampicillin and chloramphenicol for plasmid-containing strains, or in M9 minimal medium containing 0.2% glucose, 0.2% arabinose, and 0.025% Casamino Acids before polyP extraction and quantification ($n = 3$; values are means ± SDs). PolyP concentrations are in terms of individual phosphate monomers. MJG870 was derived from MJG722 by removal of the kanamycin resistance cassette in $ptsI$. This allowed us to use the kanamycin-resistant pWSK129 plasmid in these experiments. MJG870 containing pWSK129 or pPPK10 does not grow in minimal glucose medium, so polyP levels were not measured for those strains in that medium.

after nutrient limitation (Fig. 4A). Strains containing ppk^* plasmids had constitutively high polyP levels, comparable in rich medium to those found in a strain expressing wild-type ppk after stress. However, polyP production by the ppk^* alleles were not uncoupled from stress regulation, and these strains accumulated extraordinarily large amounts of polyP after nutrient limitation (in some cases, greater than 7.5 μmol of polyP mg^{-1} of protein). We confirmed these results for the E245K and D230N alleles by gel electrophoresis (Fig. 4B) and observed no difference in the distribution of polyP chain lengths produced by these mutants and the wild type.

Neither *ppx* nor *phoB* is required for the increase in polyP accumulation by *ppk** alleles. PPX is the major polyP-degrading enzyme in *E. coli* (37). We hypothesized that inhibition of PPX activity by (p)ppGpp during nutrient limitation (39) might contribute to the massive accumulation of polyP after stress in ppk^*-expressing strains. To test this hypothesis, we transformed a Δppk Δppx strain with plasmids expressing wild-type, E245K, or D230N alleles of ppk and measured polyP accumulation before and

TABLE 1 Mutants of *ppk* isolated based on the ability to allow growth on glucose under polyP-dependent conditions (*ppk** alleles)

Mutation(s)	Amino acid change(s)	No. of times isolated
G733A	E245K	8
G166A	E56K	3
G517A	E173K	3
A991G	N331D	2
A719G	E240G	1
G688A	D230N	1
G733A, G1683A	E245K	1
G741A	M247I	1
G741A, G1168A	M247I, A390T	1

after stress (Fig. 5A). Deletion of *ppx* did not prevent induction of polyP synthesis or substantially increase the amount of polyP accumulated by *ppk** strains in the absence of stress, indicating that even in *ppk** strains, PPX activity is not the primary factor controlling polyP accumulation after nutrient limitation.

We transformed the same plasmids into a Δ*ppk* Δ*phoB* strain to determine whether *ppk** alleles were able to overcome the polyP synthesis defect seen in Δ*phoB* strains (Fig. 5B). For these strains, total accumulation of polyP was indeed much lower than in a *phoB*+ background, and no polyP accumulated in the absence of stress. However, there was a measureable increase in polyP after nutrient limitation when wild-type *ppk* was provided on a plasmid, and higher levels of stress-induced polyP accumulation in both the E245K and D230N *ppk** alleles, indicating that the effects of *ppk** and Δ*phoB* mutations on polyP levels are probably independent of each other.

The toxicity of *ppk alleles in rich medium is due to magnesium starvation.** As shown above, plasmids encoding *ppk** were toxic to *E. coli* growing in rich medium (LB) (Fig. 3C), suggesting that high levels of polyP have a negative effect on cellular metabolism. We hypothesized that this might be due to the ability of polyP to efficiently chelate metal ions (81). Mg^{2+} is the most abundant divalent cation in cells (82) and is limiting in peptide-based media such as LB (83). Addition of 1 mM $MgCl_2$ to LB completely rescued the growth defect of cells containing *ppk** plasmids (Fig. 6), while addition of 1 mM $CaCl_2$ had no effect. Therefore, the toxicity observed in strains
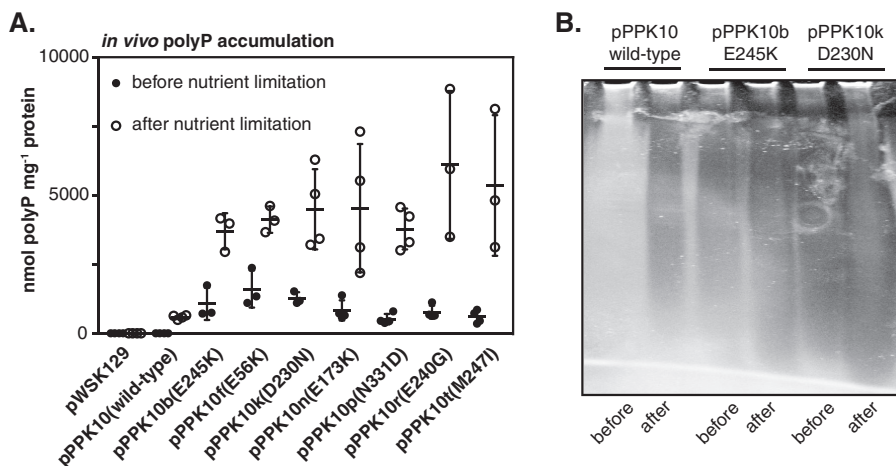

FIG 4 Strains containing *ppk** mutant plasmids accumulate very high levels of polyP *in vivo*. (A) *E. coli* Δ*ppk* containing the indicated plasmids was grown at 37°C to an A_{600} of 0.25 to 0.3 in LB containing kanamycin and then shifted for 2 h to MOPS minimal medium with no amino acids, 4 g liter^{-1} of glucose, and 0.1 mM K_2HPO_4 (*n* = 3 or 4; values are means ± SDs). PolyP concentrations are in terms of individual phosphate monomers. (B) Aliquots of GITC-lysed cells (7.5 μl; 1:10 diluted) from strains grown as described above were separated on 15% acrylamide TBE-urea gels and negative stained for polyP with DAPI. The gel is representative of the results of three independent experiments.
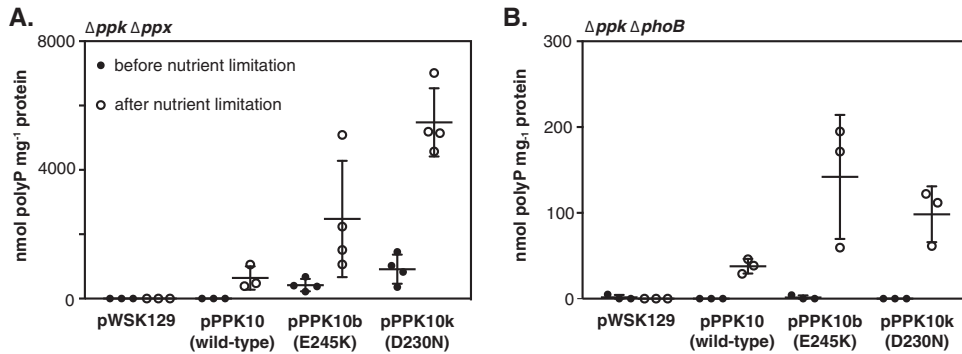
FIG 5 Neither *ppx* nor *phoB* is required for enhanced polyP synthesis by *ppk** alleles. *E. coli* Δ*ppk* Δ*ppx* (A) or Δ*ppk* Δ*phoB* (B) strains containing the indicated plasmids were grown at 37°C to an A_{600} of 0.25 to 0.3 in LB containing kanamycin and then shifted for 2 h to MOPS minimal medium with no amino acids, 4 g liter^{-1} of glucose, and 0.1 mM K$_2$HPO$_4$ (n = 3 or 4; values are means $\pm$ SDs). PolyP concentrations are in terms of individual phosphate monomers.

expressing *ppk** was almost certainly due to sequestration of Mg in biologically unavailable polyP complexes.

ppk* alleles do not encode hyperactive enzymes. The simplest hypothesis to explain the enhanced polyP levels in strains expressing *ppk** alleles is that these mutants encode very highly active PPK enzyme variants, which would themselves have valuable biotechnological applications. We therefore purified the seven PPK* variant proteins and measured their specific activity for polyP synthesis *in vitro*. Surprisingly, while PPK^{E173K} was roughly twice as active as the wild type, the rates of polyP synthesis by most variants were not dramatically different from that of the wild-type protein
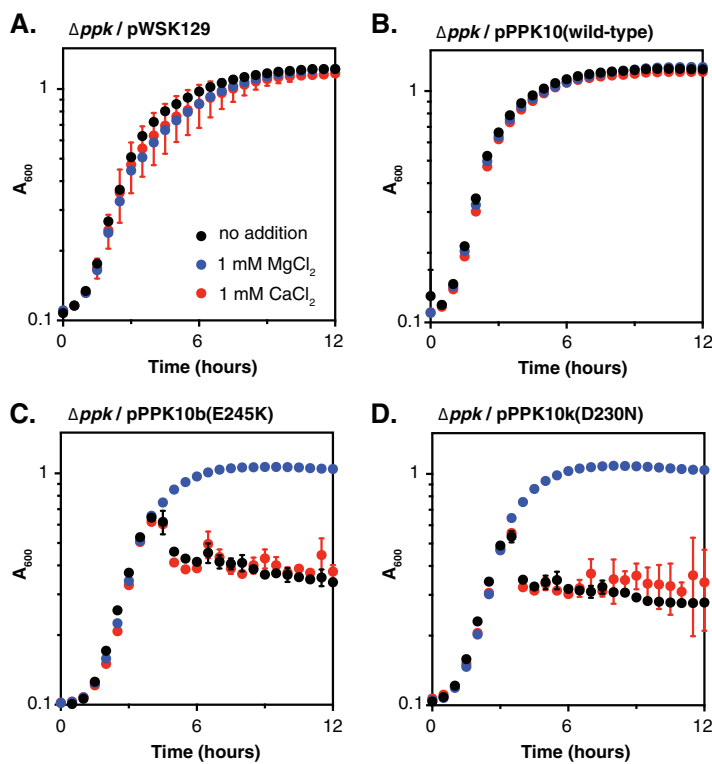

FIG 6 The toxicity of *ppk** plasmids is due to magnesium sequestration. Overnight cultures of *E. coli* Δ*ppk* containing pWSK129 (A), pPPK10 (B), pPPK10b (C), or pPPK10k (D) were diluted to an A_{600} of 0.1 in LB containing kanamycin and the indicated salts. Cultures were incubated with shaking at 37°C in a Tecan Infinite M1000 plate reader (n = 3; values are means $\pm$ SDs).

A. *in vitro* polyP kinase activity

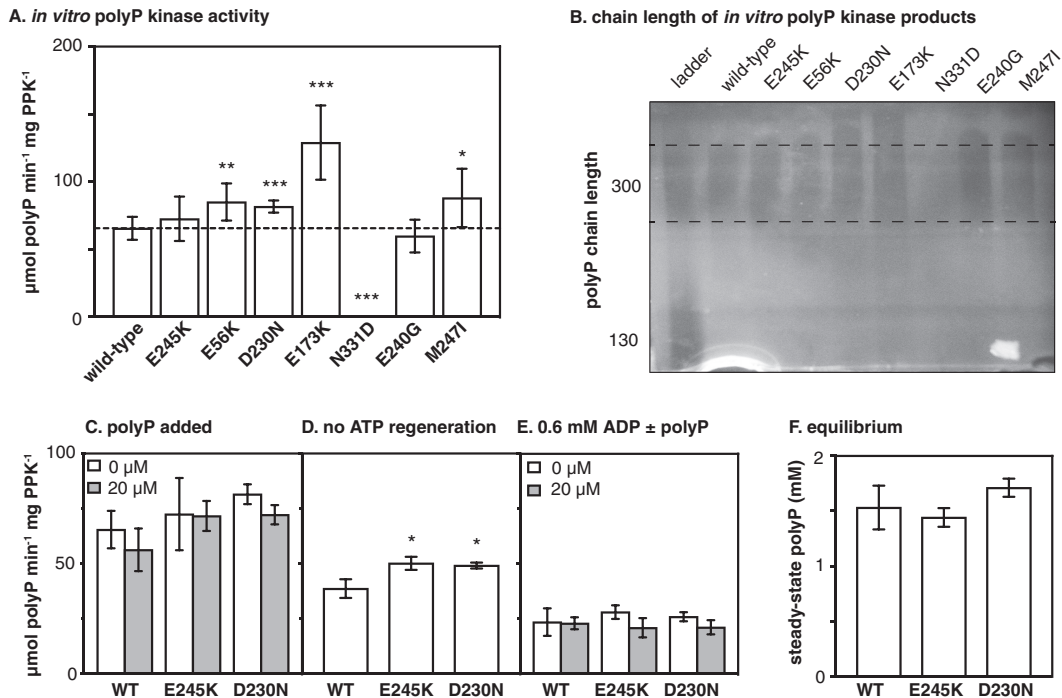**B. chain length of *in vitro* polyP kinase products**

FIG 7 *ppk** mutants do not encode hyperactive enzymes. (A) The specific activities of PPK wild-type and variant enzymes for polyP synthesis were determined *in vitro* ($n = 6$ to 12; values are means ± SDs). Asterisks indicate activities significantly different from that of wild-type enzyme (Student's *t* test; *, $P < 0.05$; **, $P < 0.01$; ***, $P < 0.001$). (B) Products of polyP synthesis reactions were separated by gel electrophoresis and visualized by negative DAPI staining. Dashed lines delineate the distribution of chain lengths produced by wild-type PPK. This gel is representative of results from 3 independent experiments. (C) The specific activities of PPK wild-type, E245K, and D230N enzymes for polyP synthesis were determined *in vitro* in the presence or absence of 20 μM polyP ($n = 3$ to 12; values are means ± SDs). (D) The specific activities of PPK wild-type, E245K, and D230N enzymes for polyP synthesis were determined *in vitro* in the absence of the creatine kinase ATP regeneration system ($n = 3$; values are means ± SDs). Asterisks indicate activities significantly different from that of wild-type enzyme (Student's *t* test; *, $P < 0.05$). (E) The specific activities of PPK wild-type, E245K, and D230N enzymes for polyP synthesis was determined *in vitro* in the absence of the creatine kinase ATP regeneration system and the presence of 0.6 mM ADP with or without 20 μM polyP ($n = 3$ or 4; values are means ± SDs). (F) Reaction mixtures (125 μl) containing 5 nM PPK, 50 mM HEPES-KOH (pH 7.5), 50 mM ammonium sulfate, 5 mM $MgCl_2$, and 6 mM MgATP were incubated overnight at 37°C to allow them to reach equilibrium ($n = 6$; values are means ± SDs).

(Fig. 7A). PPK^N331D overexpressed very poorly, and we were unable to detect any *in vitro* polyP kinase activity for this protein. The 4′,6-diamidino-2-phenylindole (DAPI) fluorescence-based polyP detection method we used in these *in vitro* assays is reported to be unaffected by polyP chain length (84), but we found that it was less sensitive for detecting extremely short polyP chains (14 phosphate units [Fig. S3]). We therefore separated the products of *in vitro* PPK and PPK* reactions on gels to determine whether PPK* enzymes produced polyP of a significantly different size than wild-type PPK *in vitro*. The bulk of the polyP produced *in vitro* by all of the PPK enzymes was 300 units long or longer (Fig. 7B), suggesting that our activity measurements were not likely to be affected by the sensitivity of the DAPI fluorescence detection method. However, we did observe that some of the PPK* proteins produced a distribution of polyP containing chain lengths slightly longer than that produced by the wild type. This was most noticeable with the PPK^D230N and PPK^E173K variants and may indicate that these variants have somewhat greater processivity than the wild-type enzyme. This was not observed for all PPK* variants, however, and the increases in both specific activity and chain length were modest, suggesting that the dramatic increases in *in vivo* polyP accumulation in *ppk** strains (Fig. 3 and 4) were not likely to be due to increases in the inherent polyP kinase activity or processivity of PPK. Illustrating this most clearly is the PPK^E245K variant, which leads to very high polyP accumulation *in vivo* but was not different from the wild type in either activity or chain length of polyP produced *in vitro* (Fig. 7A and B).

TABLE 2 Kinetic constants for the polyP-synthesizing activity of PPK and PPK* variants[a]

PPK form	K_m for ATP (mM)	K_i for ADP (mM)
Wild type	2.07 ± 0.41	0.156 ± 0.02
E245K variant	2.08 ± 0.48	0.144 ± 0.02
D230N variant	2.06 ± 0.66	0.135 ± 0.03

[a]There were no significant differences ($P < 0.05$) between the values for the wild-type and mutant proteins (Student's t test). Values are means ± SDs from 4 experiments.

The *in vitro* reaction conditions used in these assays do not necessarily reproduce the conditions PPK experiences *in vivo*, which include, for example, ATP, ADP, and polyP. We therefore adjusted the polyP-synthesizing reaction conditions to try to identify more physiological conditions under which PPK* activity may differ from that of the wild-type enzyme. First, we added polyP to PPK reactions to determine whether there was any difference in synthesis rates when elongating existing chains rather than synthesizing polyP from scratch. Addition of polyP to PPK, PPK^E245K, or PPK^D230N had no significant effect on the specific activity of these enzymes (Fig. 7C). We next removed the ADP-eliminating creatine kinase ATP regeneration system from the reactions. As expected, this reduced activity, since ADP is a potent competitive inhibitor of PPK (8). Under these conditions, both PPK^E245K and PPK^D230N had slightly, but significantly (Student's t test, $P < 0.05$), higher initial rates of polyP synthesis than wild-type PPK (Fig. 7D). However, when we added 0.6 mM ADP, approximating the *in vivo* ADP concentration in *E. coli* (85), wild-type PPK, PPK^E245K, and PPK^D230N were all inhibited to the same extent in either the absence or presence of polyP (Fig. 7E). There was no difference in the amount or chain length of polyP accumulated in PPK, PPK^E245K, and PPK^D230N reactions allowed to come to equilibrium in the absence of ATP regeneration (Fig. 7F; see also Fig. S4). To more quantitatively measure the effect of ADP on PPK and PPK* enzymes, we determined the K_m for ATP and the inhibition constant (K_i) for ADP for PPK, PPK^E245K, and PPK^D230N, and we found that none of these values differed significantly from those of the wild-type enzyme (Table 2). We have so far been unable to identify any differences in *in vitro* enzyme activity that explain the dramatic increases in *in vivo* polyP levels in strains expressing *ppk**.

ppk* mutations alter amino acids distant from the PPK active site. Consistent with the modest changes in *in vitro* enzyme activity, when we mapped the amino acids mutated in *ppk** alleles onto the three-dimensional structure of PPK (PDB accession code 1XDP) (86), none were located in the predicted active site (Fig. 8A). The majority of the mutated residues (5 of 7) instead are found in the head domain within a radius of 12 Å of each other, with 4 of these residues (D230, E240, E245, and M247) found in the extension between α-strands s7 and s8. D230 is located at the base of the extension, while the three remaining residues are found on the distal loop (residues 239 to 251) of the extension, with E245 protruding outward. E56 concludes this cluster of five mutations and is partially buried at the interface between the head and the N-terminal and C2 domains, where it forms a salt bridge with R616. The other two mutated residues (E173 and N331) are located on the surface of the head and C1 domains, respectively. These two mutations (E173K and N331D) resulted in more significant changes in *in vitro* activity, albeit in opposite directions (Fig. 7A). Of the amino acids mutated in *ppk** alleles, D230 is the most broadly conserved among bacterial PPK homologs, followed by E173 (Fig. 9). The most common nucleotide mutation we isolated (9 of 21) was G733A, resulting in the PPK^E245K variant protein.

The oligomeric state of PPK has previously been described as a dimer (86, 87) and as a tetramer (8, 87). The asymmetric unit of the crystal form determined by Zhu et al. contains a dimer of PPK (chains A and B) with a buried surface area of 1,678 Å². Amino acids E173 and N331 are found on complementary surfaces within this dimeric interface, with each residue contributed by a separate monomer in the local interface (e.g., chain A residue E173 and chain B residue N331 [Fig. S5]). These surfaces are duplicated on a second dimeric interface across the approximate 2-fold axis of symmetry that
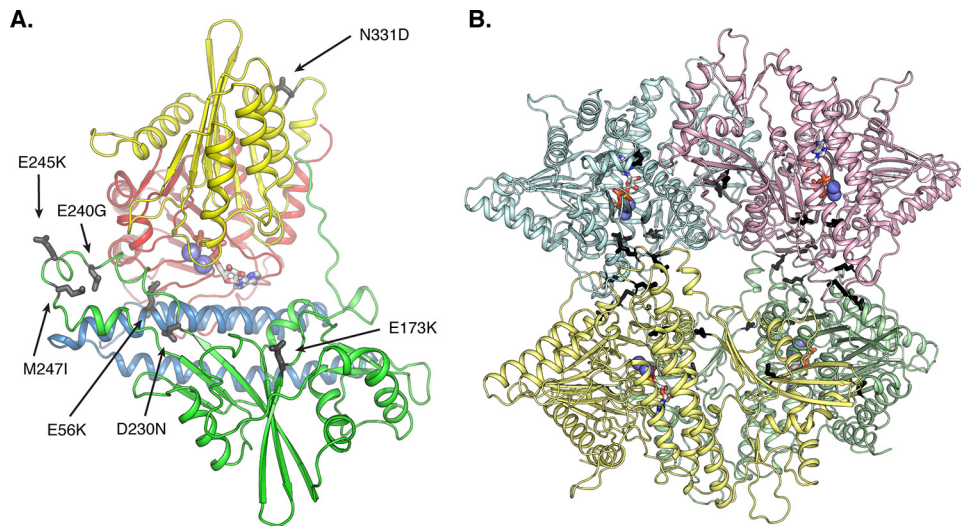
FIG 8 Location of amino acids mutated in PPK* variants in the PPK crystal structure reported by Zhu et al. (86). (A) The monomer of the PPK is shown with the N-terminal domain (residues 2 to 106) colored in blue, the head domain (residues 107 to 321) in green, the C-terminal domain C1 (residues 322 to 502) in yellow, and domain C2 (residues 503 to 687) in red. (B) The tetrameric arrangement of PPK is shown, with each monomer colored in light shades of pink (chain A), blue (chain B), yellow (chain A') and green (chain B'). In both panels A and B, side chains at sites of mutation are shown as a stick model (gray), the ATP analog(s) is shown as a stick model, and Mg^{2+} ions are shown as spheres (slate).

relates chain A and B. Portions of the head and C1 domains solely contribute to the interface of the dimer. We visually analyzed the PPK structure of Zhu et al. in the context of the tetragonal crystal system ($P4_22_12$) with COOT (88) and more thoroughly with PISA (89). A clear tetrameric assembly (Fig. 8B) can be observed between the asymmetric unit content and equivalent chains (designated A' and B') generated by symmetry operation ($-x, -y - 1, z$). This PPK assembly has 222-point symmetry and is built through four dimeric interactions (between chains A/B, A'/B, A'/B', and A/B') with comparable buried surface areas of 1678 and 1438 Å² between the two unique dimeric interfaces (A/B and A'/B). The dimeric interface formed between chains A'/B (Fig. S5) is unique as it shows the intersection of three of the four PPK domains (head, C1, and C2). The distal part of the extension between strands s7 and s8 (head domain), containing sites of mutation E240, E245, and M247, is a prominent feature which extends across the dimeric interface to contact the surface of domain C1. Amino acids E240 and M247 appear to play roles in formation of the structure of the distal loop, placing the negatively charged E245 exposed on the tip of the extension. This positions E245 among a cluster of positively charged amino acids (K370, R451, and R485) across this dimer interface within an average distance of 3.4 Å. Mutations E240G and M247I could disrupt the structure of the extension, while mutation E245K could disrupt the electrostatic interaction between monomers, potentially causing loss of dimer formation.

DISCUSSION

We have developed a novel genetic system that allowed us to isolate *ppk** mutants that lead to dramatically enhanced polyP accumulation *in vivo* (Fig. 3 and 4). Previous mutational analyses of *ppk*, primarily using alanine scanning, have identified conserved residues essential for activity (87, 90), but in the absence of a specific and easily measured phenotype for polyP accumulation, no mutations of *ppk* leading to enhanced polyP synthesis have been reported before. Mutations inactivating the phosphate uptake repressor PhoU do lead to increased polyP, but these mutants suffer from genetic instability (58, 59). Previous attempts to engineer *E. coli* to stably produce high levels of polyP by overexpressing wild-type PPK have generally resulted in relatively modest (2- to 8-fold) increases in polyP content (32–35).
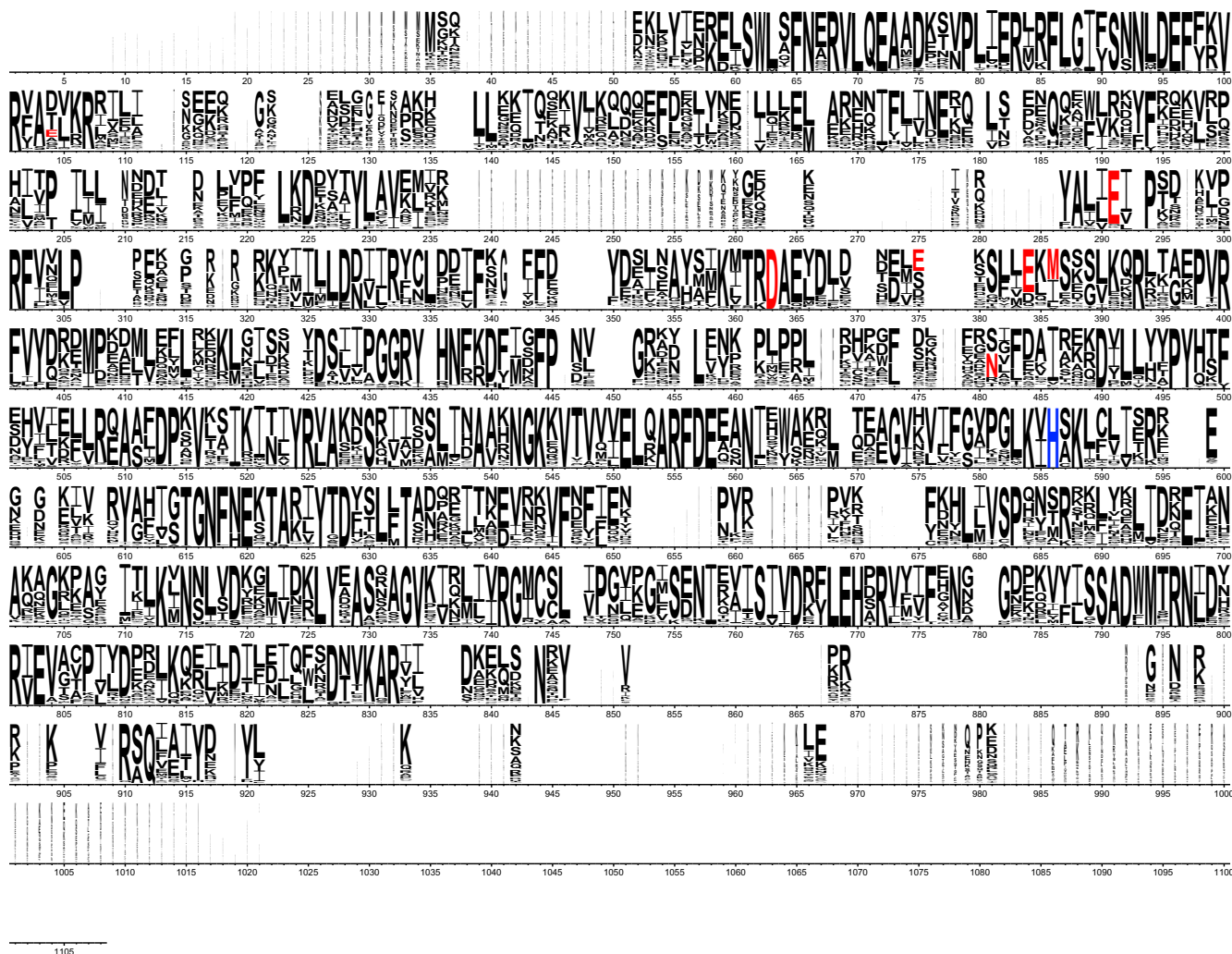
FIG 9 Alignment of PPK homologs from 854 bacterial species (BLAST E value $< 1 \times 10^{-150}$ compared to *E. coli* PPK; one homolog per species). The position of each mutated *E. coli* amino acid in the alignment is as follows: E56, position 104; E173, position 291; D230, position 363; E240, position 375; E245, position 384; M247, position 386; and N331, position 481. The autophosphorylated active-site histidine (H435 in *E. coli*; position 586 in the alignment) is indicated in blue.

The high levels of polyP produced by *ppk** mutants inhibited growth of *E. coli* in Mg-limited medium (Fig. 6), indicating that polyP is an efficient chelator of cytoplasmic Mg. This not only indicates that adding Mg should improve the growth of bacteria engineered to produce high levels of polyP in biotechnological settings but also may be physiologically relevant under natural conditions in which bacteria produce substantial amounts of polyP. Growth arrest is common under such conditions (14, 38, 40), and slow growth is itself associated with increases in stress tolerance (91). Mg sequestration could therefore be a mechanism contributing to polyP-dependent stress resistance.

The seven *ppk** mutations described here are predominantly found at or near points of interaction in the formation of larger ordered oligomers of PPK (Fig. 8; see also Fig. S5). Disruption of these surfaces by mutation could disrupt dimer and subsequently tetramer formation. The dimer previously described by Zhu et al. (86) is complemented by a second dimeric arrangement previously not described but observed in the lattice symmetry of the crystal (PDB accession code 1XDP). Collectively, the two distinct dimeric arrangements come together to form a PPK homotetramer with a combined buried surface area of 6,232 Å², a 2.7-fold increase over the dimer alone. While it is

possible that mutations disrupting dimer and tetramer formation could enhance PPK activity, it is not immediately obvious how they result in PPK enzymes that cause high levels of polyP accumulation *in vivo* but whose *in vitro* activity seems unaffected. We think the most likely explanation is that there is a factor or factors present *in vivo* which inhibits PPK activity or stability but is not present in our *in vitro* reactions and that the *ppk** mutations disrupt these *in vivo* control factors. We are currently pursuing experiments to determine the mechanism by which *ppk** mutations lead to increased polyP levels, including attempts to identify proteins or small molecules that may interact with PPK to limit its activity *in vivo*.

The existence of *ppk** alleles, which lead to substantially higher baseline levels of polyP *in vivo* but do not uncouple polyP synthesis from stress induction (Fig. 4), suggests that there must be at least three independent control elements able to affect polyP accumulation in *E. coli* in addition to inhibition of PPX by (p)ppGpp or redox stress. First, deletion of *phoB* dramatically decreases polyP synthesis, both in the wild type and *ppk** mutants (Fig. 1 and 5). A *phoB* mutant does not express the *pstSCAB-phoU* operon (92) and therefore lacks the high-affinity Pst phosphate uptake system. This, combined with the observation that *phoU* mutants constitutively accumulate phosphate and synthesize high levels of polyP (58, 59) and the elevated polyP levels found in stationary-phase *E. coli* grown in medium containing excess phosphate (93), indicates that phosphate import and availability play an important role in permitting polyP synthesis. Second, *ppk** mutations do not appear to encode hyperactive PPK enzymes but rather lead to an overall increase in polyP accumulation *in vivo* in both the presence and absence of stress (Fig. 4). This suggests that the *ppk** mutations have disrupted PPK-repressing interactions that normally prevent PPK from acting to its full polyP-synthesizing potential. Finally, neither deletion of *phoB* nor expression of *ppk** alleles prevented activation of polyP accumulation after stress (Fig. 4 and 5), indicating that there must be still another mechanism or mechanisms by which stress signals are transmitted to PPK.

Compared to some other bacteria, *E. coli* has a relatively simple set of genes involved in polyP metabolism. The *ppk-ppx* operon encodes the only copies of PPK and PPX in the *E. coli* genome and does not appear to be transcriptionally upregulated by stress in *E. coli*, although our data (Fig. 1B) hint that polyP or PPK may play some role in *ppk* expression under nonstress growth conditions. In contrast, in *P. aeruginosa*, for example, expression of *ppk* and *ppx* are distinctly differentially regulated (94), and the genome also encodes three copies of the alternative polyP kinase PPK2 (10, 36). Some bacteria (e.g., *Corynebacterium glutamicum* or *Chlorobium tepidum*) have more than one PPX homolog with different specificities for polyP of different lengths (95, 96). *E. coli* therefore represents a relatively straightforward model organism for probing the regulation of polyP synthesis, and given the high conservation of PPK in general and some of the residues mutated in *ppk** alleles in particular, we expect that insights we gain into control of PPK activity and polyP synthesis in *E. coli* will be applicable to a broad range of bacterial species.

While this paper was under review, Wang et al. (97) reported that modest overexpression of PPK in the environmental bacterium *Citrobacter freundii* resulted in very high polyP accumulation. This was surprising to us, since similar overexpression experiments with *E. coli* have not resulted in such dramatic increases in polyP content (32–35). PPKs from *E. coli* and *C. freundii* are 96% identical, but the major difference is that the *C. freundii* PPK has a glutamate and a lysine residue in positions 327 and 328, where *E. coli* PPK has much less strongly charged alanine and glutamine residues. These residues are very near N331 in the predicted interface between monomers, and we hypothesize that they may result in PPK*-like properties for *C. freundii* PPK. Intriguingly, in PPK homologs from polyP-accumulating EBPR bacteria ("*Candidatus* Accumulibacter" spp.) (31), the residue equivalent to D230 is highly conserved as an N residue, and the distal loop sequence (containing E240, E245, and M247 in *E. coli* PPK) is quite different from that in *E. coli*, suggesting that perhaps "*Candidatus* Accumulibacter" also naturally possesses highly active "*ppk**" genes.

In conclusion, the work presented here identifies conserved residues in PPK responsible for preventing overproduction of polyP *in vivo*, (possibly by modulating interactions between monomers of PPK), shows that high polyP levels can lead to Mg starvation in Mg-limited medium, provides new insights into the control of bacterial polyP synthesis, and provides a simple strategy for dramatically enhancing the polyP content of bacterial cells.

MATERIALS AND METHODS

Bacterial strains, growth conditions, and molecular methods. All strains and plasmids used in this study are listed in Table 3. DNA manipulations were carried out by standard methods (98) in *E. coli* cloning strains XL1-Blue (Stratagene) and DH5α (Invitrogen). PCR and sequencing primers were designed with Web Primer (https://www.yeastgenome.org/cgi-bin/web-primer). Mutagenic primers were designed with PrimerX (http://www.bioinformatics.org/primerx/index.htm). *E. coli* was grown in lysogeny broth (LB) (99) or M9 minimal medium (98) containing 0.2% glucose, 0.2% arabinose, and 0.025% Casamino Acids. Antibiotics were added when appropriate: ampicillin (100 mg ml^{-1}), kanamycin (12.5 or 50 mg ml^{-1}), chloramphenicol (17 or 34 mg ml^{-1}), or gentamicin (30 mg ml^{-1}). To induce polyP production by nutrient limitation (38, 100), *E. coli* was grown to an A_{600} of 0.25 to 0.3 in LB at 37°C with shaking, at which point 5 ml was spun down (5 min at 4,696 × *g* and room temperature), rinsed once with 5 ml of phosphate-buffered saline (PBS), resuspended in 5 ml of MOPS minimal medium (Teknova) containing 4 g l^{-1} of glucose and 0.1 mM K$_2$HPO$_4$, and then incubated for a further 2 h at 37°C with shaking.

Sequence analysis. Gene and protein sequences were obtained from the Integrated Microbial Genomes database (101). Custom Python scripts using the Biopython 1.67 toolkit (102) were used to search for and sort PPK homologs from the National Center for Biotechnology Information database (https://www.ncbi.nlm.nih.gov), filtering them to obtain a list containing one homolog per bacterial species. Sequence alignments were performed using MUSCLE 3.8 (103), and sequence logos were generated using WebLogo 3.5 (104).

Strain construction. P1*vir* transduction (105) was used to move the *phoB763*::*kan*$^+$ allele from the Keio collection (106) into *E. coli* wild-type strain MG1655 (F$^-$ *rph-1 ilvG rfb-50*) (107), generating strain MJG214 (*phoB763*::*kan*$^+$). The kanamycin resistance cassette was resolved as described previously (76), yielding strain MJG227 (Δ*phoB763*). Strain MJG452 (*araA*::*cat*$^+$) was generated by P1*vir* transduction of the *araA*::*cat*$^+$ allele from strain MT555 (Δ*malE* Δ*hsdR araA*::*cat*$^+$) (a gift from James Bardwell, University of Michigan) into MG1655. The chloramphenicol resistance cassette was resolved, yielding strain MJG621 (Δ*araA*). The *ppk-ppx* operon of this strain was replaced with a chloramphenicol resistance cassette (76) using primers 5′ CAT AAT ATC CAG GCA GTG TCC CGT GAA TAA AAC GGA GTA AAA GTG GTA ATG GTG TAG GCT GGA GCT GCT TC 3′ and 5′ AAG TGC CTG AAT AAT GCG GGC CGA CAT TTC TCG TCG GCC CGC AAA GTA TTA CAT ATG GAA ATC CTC CTT AG 3′ (14), yielding strain MJG670 (Δ*araA ppk-ppx*::*cat*$^+$), and then resolved to give strain MJG671 (Δ*araA* Δ*ppk* Δ*ppx*). P1*vir* transduction was used to move the *glk-726*::*kan*$^+$ allele from the Keio collection into MJG671 to give strain MJG684 (Δ*araA* Δ*ppk* Δ*ppx glk-726*::*kan*$^+$), which was then resolved to give strain MJG692 (Δ*araA* Δ*ppk* Δ*ppx* Δ*glk-726*). P1*vir* transduction was used to move the *galR762*::*kan*$^+$ allele from the Keio collection into MJG671 and MJG692 to give strains MJG717 (Δ*araA* Δ*ppk* Δ*ppx galR762*::*kan*$^+$) and MJG718 (Δ*araA* Δ*ppk* Δ*ppx* Δ*glk-726 galR762*::*kan*$^+$), which were then resolved to give strains MJG719 (Δ*araA* Δ*ppk* Δ*ppx* Δ*galR762*) and MJG720 (Δ*araA* Δ*ppk* Δ*ppx* Δ*glk-726* Δ*galR762*). P1*vir* transduction was used to move the *ptsI745*::*kan*$^+$ allele from the Keio collection into MJG719 and MJG720 to give strains MJG721 (Δ*araA* Δ*ppk* Δ*ppx* Δ*galR762 ptsI745*::*kan*$^+$) and MJG722 (Δ*araA* Δ*ppk* Δ*ppx* Δ*glk-726* Δ*galR762 ptsI745*::*kan*$^+$), followed by resolution of the kanamycin resistance cassettes to yield strains MJG739 (Δ*araA* Δ*ppk* Δ*ppx* Δ*galR762* Δ*ptsI745*) and MJG740 (Δ*araA* Δ*ppk* Δ*ppx* Δ*glk-726* Δ*galR762* Δ*ptsI745*). P1*vir* transduction was used to move *ppk-ppx*::*cat*$^+$ from MJG670 into strain MG1655, yielding strain MJG1094 (*ppk-ppx*::*cat*$^+$), which was then resolved to give strain MJG1115 (Δ*ppk* Δ*ppx*). P1*vir* transduction was used to move the *phoB763*::*kan*$^+$ allele from the Keio collection into strain MJG224 (Δ*ppk*), yielding strain MJG1095 (Δ*ppk phoB763*::*kan*$^+$), which was resolved to give strain MJG1117 (Δ*ppk* Δ*phoB763*). All chromosomal mutations were confirmed by PCR.

Plasmid construction. The *ppgK* (*all1371*) coding sequence (717 bp) from *Anabaena* sp. strain PCC 7120 (17) was codon optimized for expression in *E. coli* (GenScript), yielding a *ppgK*$^{opt.}$ allele encoding the wild-type PPGK amino acid sequence in plasmid pPPGK1. The *ppgK*$^{opt.}$ coding sequence was subcloned, along with an efficient *E. coli* ribosome binding site (5′ AAG GAG ATA TAC AT 3′) derived from pET-11a (108) (EMD Millipore), into the KpnI and HindIII sites of plasmid pBAD33 (72) to yield plasmid pPPGK6.

The *glk* coding sequence (966 bp) plus 14 bp of 5′ sequence was amplified from *E. coli* MG1655 genomic DNA with primers 5′ TTC GAA TTC GGA GCA GTT GAA GAA TGA CAA AG 3′ and 5′ AGA TCT AGA TTA CAG AAT GTG ACC TAA GGT CTG G 3′ and cloned into the EcoRI and XbaI sites of plasmid pBAD18 (72) to yield plasmid pGLK1.

The *ppk* coding sequence (2,067 bp) plus 171 bp of upstream sequence was amplified from *E. coli* MG1655 genomic DNA with primers 5′ ACC GGT ACC TAC CCC CGT AAT TAA AGC G 3′ and 5′ AGA TCT AGA TTA TTC AGG TTG TTC GAG TGA TTT G 3′ and cloned into the KpnI and XbaI sites of plasmid pWSK129 (79) to yield plasmid pPPK10. To ensure that *ppk* expression was driven only by its native promoter, *ppk* was cloned in the opposite orientation from the *lac* promoter of pWSK129.

The *uidA* (*gusA*) coding sequence (1,812 bp) was amplified from *E. coli* MG1655 genomic DNA with primers 5′ CTT AAG CTT ATG TTA CGT CCT GTA GAA ACC CCA 3′ and 5′ ACG GCT AGC TCA TTG TTT GCC TCC CTG CT 3′ and cloned into the HindIII and NheI sites of plasmid pSRKGm (109) to yield plasmid

TABLE 3 Strains and plasmids used in this study[a]

Strain or plasmid	Marker(s)	Relevant genotype	Source or reference
E. coli strains			
BL21(DE3)		F$^-$ *ompT gal dcm lon hsdSB* (r$_B^-$ m$_B^-$) λ(DE3 [*lacI lacUV5*-T7 gene 1 *ind1 sam7 nin5*])	EMD Millipore
XL1-Blue	Tc^r Nx^r	*endA1 gyrA96* (Nx^r) *thi-1 recA1 relA1 lac glnV44* F′[::Tn*10* (*tet$^+$*) *proAB$^+$ lacI*$_q$ Δ(*lacZ*)M15] *hsdR17* (r$_K^-$ m$_K^+$)	Agilent Technologies
XL1-Red	Tc^r Nx^r	*endA1 gyrA96* (Nx^r) *thi-1 relA1 lac glnV44 hsdR17* (r$_K^-$ m$_K^+$) *mutS mutT mutD5* Tn*10* (*tet$^+$*)	Agilent Technologies
DH5α		F$^-$ λ$^-$ φ80*lacZ*ΔM15 Δ(*lacZYA-argF*)U169 *recA1 endA1 hsdR17* (r$_K^-$ m$_K^+$) *phoA supE44 thi-1 gyrA96 relA1*	Invitrogen
MT555	Cm^r	Δ*malE* Δ*hsdR araA::cat$^+$*	J. Bardwell
MG1655		F$^-$ λ$^-$ *rph-1 ilvG rfb-50*	107
MJG214	Kn^r	F$^-$ λ$^-$ *rph-1 ilvG rfb-50 phoB763::kan$^+$*	
MJG224		F$^-$ λ$^-$ *rph-1 ilvG rfb-50* Δ*ppk*	14
MJG227		F$^-$ λ$^-$ *rph-1 ilvG rfb-50* Δ*phoB763*	
MJG315		F$^-$ λ$^-$ *rph-1 ilvG rfb-50* Δ*ppx*	14
MJG452	Cm^r	F$^-$ λ$^-$ *rph-1 ilvG rfb-50 araA::cat$^+$*	
MJG621		F$^-$ λ$^-$ *rph-1 ilvG rfb-50* Δ*araA*	
MJG670	Cm^r	F$^-$ λ$^-$ *rph-1 ilvG rfb-50* Δ*araA ppk-ppx::cat$^+$*	
MJG671		F$^-$ λ$^-$ *rph-1 ilvG rfb-50* Δ*araA* Δ*ppk* Δ*ppx*	
MJG684	Kn^r	F$^-$ λ$^-$ *rph-1 ilvG rfb-50* Δ*araA* Δ*ppk* Δ*ppx glk-726::kan$^+$*	
MJG692		F$^-$ λ$^-$ *rph-1 ilvG rfb-50* Δ*araA* Δ*ppk* Δ*ppx* Δ*glk-726*	
MJG717	Kn^r	F$^-$ *rph-1 ilvG rfb-50* Δ*araA* Δ*ppk* Δ*ppx galR762::kan$^+$*	
MJG718	Kn^r	F$^-$ *rph-1 ilvG rfb-50* Δ*araA* Δ*ppk* Δ*ppx* Δ*glk-726 galR762::kan$^+$*	
MJG719		F$^-$ *rph-1 ilvG rfb-50* Δ*araA* Δ*ppk* Δ*ppx* Δ*galR762*	
MJG720		F$^-$ *rph-1 ilvG rfb-50* Δ*araA* Δ*ppk* Δ*ppx* Δ*glk-726* Δ*galR762*	
MJG721	Kn^r	F$^-$ *rph-1 ilvG rfb-50* Δ*araA* Δ*ppk* Δ*ppx* Δ*galR762 ptsI745::kan$^+$*	
MJG722	Kn^r	F$^-$ *rph-1 ilvG rfb-50* Δ*araA* Δ*ppk* Δ*ppx* Δ*glk-726* Δ*galR762 ptsI745::kan$^+$*	
MJG739		F$^-$ *rph-1 ilvG rfb-50* Δ*araA* Δ*ppk* Δ*ppx* Δ*galR762* Δ*ptsI745*	
MJG740		F$^-$ *rph-1 ilvG rfb-50* Δ*araA* Δ*ppk* Δ*ppx* Δ*glk-726* Δ*galR762* Δ*ptsI745*	
MJG1094	Cm^r	F$^-$ *rph-1 ilvG rfb-50 ppk-ppx::cat$^+$*	
MJG1095	Kn^r	F$^-$ *rph-1 ilvG rfb-50* Δ*ppk phoB763::kan$^+$*	
MJG1115		F$^-$ *rph-1 ilvG rfb-50* Δ*ppk* Δ*ppx*	
MJG1117		F$^-$ *rph-1 ilvG rfb-50* Δ*ppk* Δ*phoB763*	
Plasmids			
pET-11a	Ap^r		EMD Millipore
pBAD33	Cm^r		72
pBAD18	Ap^r		72
pWSK129	Kn^r		79
pSRKGm	Gm^r		109
pPPK2	Ap^r	*ppk$^+$*-His$_6$	14
pPPK7	Ap^r	*ppk$^+$*	14
pGLK1	Ap^r	*glk$^+$*	
pPPGK1	Ap^r	*ppgK$^{opt.}$*	
pPPGK6	Cm^r	*ppgK$^{opt.}$*	
pPPK10	Kn^r	*ppk$^+$*	
pPPK10a	Kn^r	*ppk$^{G733A, G1683A}$* (encoding PPK^{E245K})	
pPPK10b	Kn^r	*ppk^{G733A}* (encoding PPK^{E245K})	
pPPK10c	Kn^r	*ppk^{G733A}* (encoding PPK^{E245K})	
pPPK10d	Kn^r	*ppk^{A991G}* (encoding PPK^{N331D})	
pPPK10e	Kn^r	*ppk^{G733A}* (encoding PPK^{E245K})	
pPPK10f	Kn^r	*ppk^{G166A}* (encoding PPK^{E56K})	
pPPK10g	Kn^r	*ppk^{G166A}* (encoding PPK^{E56K})	
pPPK10h	Kn^r	*ppk^{G733A}* (encoding PPK^{E245K})	
pPPK10i	Kn^r	*ppk^{G733A}* (encoding PPK^{E245K})	
pPPK10j	Kn^r	*ppk^{G517A}* (encoding PPK^{E173K})	
pPPK10k	Kn^r	*ppk^{G688A}* (encoding PPK^{D230N})	
pPPK10l	Kn^r	*ppk$^{G741A, G1168A}$* (encoding PPK$^{M247I, A390T}$)	
pPPK10 m	Kn^r	*ppk^{G166A}* (encoding PPK^{E56K})	
pPPK10n	Kn^r	*ppk^{G517A}* (encoding PPK^{E173K})	
pPPK10o	Kn^r	*ppk^{G733A}* (encoding PPK^{E245K})	
pPPK10p	Kn^r	*ppk^{A991G}* (encoding PPK^{N331D})	
pPPK10q	Kn^r	*ppk^{G733A}* (encoding PPK^{E245K})	
pPPK10r	Kn^r	*ppk^{A719G}* (encoding PPK^{E240G})	
pPPK10s	Kn^r	*ppk^{G517A}* (encoding PPK^{E173K})	

(Continued on next page)

TABLE 3 (Continued)

Strain or plasmid	Marker(s)	Relevant genotype	Source or reference
pPPK10t	Kn^r	ppk^{G741A} (encoding PPK^{M247I})	
pPPK10u	Kn^r	ppk^{G733A} (encoding PPK^{E245K})	
pPPK14	Ap^r	ppk^{G733A} (encoding PPK^{E245K}-His$_6$)	
pPPK15	Ap^r	ppk^{A719GA} (encoding PPK^{E240G}-His$_6$)	
pPPK16	Ap^r	ppk^{A991G} (encoding PPK^{N331D}-His$_6$)	
pPPK17	Ap^r	ppk^{G166A} (encoding PPK^{E56K}-His$_6$)	
pPPK18	Ap^r	ppk^{G517A} (encoding PPK^{E173K}-His$_6$)	
pPPK19	Ap^r	ppk^{G688A} (encoding PPK^{D230N}-His$_6$)	
pPPK20	Ap^r	ppk^{G741A} (encoding PPK^{M247I}-His$_6$)	
pGUSA4	Gm^r	$uidA^+$	
pGUSA5	Gm^r	P$_{ppk}$-$uidA^+$	

^{a}Unless otherwise indicated, all strains and plasmids were generated in the course of this work. Abbreviations: Tc^r, tetracycline resistance; Nx^r, nalidixic acid resistance; Cm^r, chloramphenicol resistance; Kn^r, kanamycin resistance; Sm^r, streptomycin resistance; Ap^r, ampicillin resistance; Gm^r, gentamicin resistance.

pGUSA4. The first six codons of *ppk* and 600 bp of upstream sequence were then amplified from *E. coli* MG1655 genomic DNA with primers 5′ TTC GAA TTC TTG ATT CAT GAA ATC GAC ATG TAC G 3′ and 5′ CTT AAG CTT TAG CTT TTC CTG ACC CAT TAC G 3′ and cloned into the EcoRI and HindIII sites of plasmid pGUSA4 to yield plasmid pGUSA5, in which β-glucuronidase expression is under the control of the *ppk* transcriptional and translational regulatory sequences. All plasmid constructs were confirmed by sequencing (University of Alabama at Birmingham Heflin Genomics Core).

β-Glucuronidase assays. We used standard methods (110) to measure expression of the plasmid-encoded P$_{ppk}$-*uidA* fusion by assaying β-glucuronidase activity. Cell pellets from 1 ml of culture were resuspended in 500 μl of GUS buffer (50 mM sodium phosphate [pH 7], 10 mM β-mercaptoethanol, 1 mM EDTA, 0.1% Triton X-100) and permeabilized by addition of 12.5 μl of 0.1% sodium dodecyl sulfate and 25 μl of chloroform. After prewarming to 37°C, reactions were started by addition of 12.5 μl of 4-mg ml^{-1} *p*-nitrophenyl-β-D-glucuronide in 50 mM sodium phosphate (pH 7) and stopped at appropriate time points (typically 15 min) by addition of 250 μl of 1 M Na$_2$CO$_3$. After removing particles by centrifugation (10 min at 21,100 × *g*), we measured the amount of *p*-nitrophenol product accumulated (A_{405}) in a Genesys 10S UV-visible (UV-Vis) spectrophotometer (Thermo Fisher), blanked to a no-cell control reaction. Miller units were calculated as 1,000 × [A_{405}/(A_{600} of culture × milliliters of culture added to the reaction × reaction time, in minutes)].

Random mutagenesis of *ppk*. Plasmid pPPK10 was randomly mutated by one passage through the *mutS mutT mutD* mutator strain XL1-Red (Agilent Technologies), according to the manufacturer's instructions. The resulting pool of mutagenized plasmids was electroporated into strain MJG870 (MJG740/pPPGK6), spread on M9 agar containing 0.2% glucose, 0.2% arabinose, and 0.025% Casamino Acids, and incubated 2 days at 37°C. Robustly growing colonies were picked and streaked for isolation on the same medium. Plasmid preps from these isolates were retransformed into MJG740, selected for growth on LB containing chloramphenicol and kanamycin, and then streaked for isolation on M9 agar containing 0.2% glucose, 0.2% arabinose, and 0.025% Casamino Acids to confirm that the ability to grow on glucose was due to plasmid-encoded mutations. The *ppk* alleles carried by pPPK10-derived mutant plasmids were sequenced using primers 5′ GTG GCG ATA CCA TCC GTT 3′, 5′ GAA CAG TTT GGC GTG AAT 3′, 5′ CGA GCG TAC TGG CGA TTA 3′, 5′ CCA GTG GTA TCA CCC TGA 3′, 5′ CCA GCG CAT TGG GCA TAT 3′, and 5′ GCG CCA TCT CCA GCA ATA 3′. pPPK10-derived mutant plasmids were isolated from strains containing those plasmids and pPPGK6 by passaging selected strains in LB containing kanamycin and screening for loss of chloramphenicol resistance.

Site-directed mutagenesis of *ppk*. The QuikChange site-directed mutagenesis method (Agilent Technologies), modified to use a single primer and 35 cycles of amplification, was used to mutate the *ppk*$^+$ overexpression plasmid pPPK2 (14) as follows. Primer 5′ GAA GCC AGC CTG ATG AAG TTG ATG TCT TCC 3′ was used to generate plasmid pPPK14, containing a *ppk*^{G733A} allele encoding PPK^{E245K}. Primer 5′ GTG CAT GAG ATG GGA GCC AGC CTG ATG 3′ was used to generate plasmid pPPK15, containing a *ppk*^{A719G} allele encoding PPK^{E240G}. Primer 5′ GCC CAG TTC CGC GAT GGT TTT GAT GC 3′ was used to generate plasmid pPPK16, containing a *ppk*^{A991G} allele encoding PPK^{N331D}. Primer 5′ GTC CGC TTC GCT AAA CTG AAG CGA CG 3′ was used to generate plasmid pPPK17, containing a *ppk*^{G166A} allele encoding PPK^{E56K}. Primer 5′ CAT CCG TTA CGC GCT GCT GAA GAT CCC ATC AGA TAA AG 3′ was used to generate plasmid pPPK18, containing a *ppk*^{G517A} allele encoding PPK^{E173K}. Primer 5′ CAA TGA AGA TGA CCC GCA ATG CCG AAT ACG ATT TAG 3′ was used to generate plasmid pPPK19, containing a *ppk*^{G688A} allele encoding PPK^{D230N}. Primer 5′ CCT GAT GGA GTT GAT ATC TTC AGT CTT CAA G 3′ was used to generate plasmid pPPK20, containing a *ppk*^{G741A} allele encoding PPK^{M247I}.

***In vivo* polyP assay.** Intracellular polyP levels were measured by a slight modification of a previously published protocol (14). Enough cells to total approximately 50 μg of protein (typically 1 ml of a culture at an A_{600} of 0.25 to 0.3) were harvested by centrifugation, resuspended in 250 μl of GITC lysis buffer (4 M guanidine isothiocyanate, 50 mM Tris-HCl [pH 7]), and incubated for 10 min at 95°C. Protein concentration was determined by Bradford assay (Bio-Rad) of a 5-μl aliquot, and lysates were stored at −80°C. After thawing, 15 μl of 10% SDS and 250 μl of 95% ethanol were added, with vortexing between additions. The resulting mixture was applied (2 min at 2,000 × *g* and room temperature) to an EconoSpin silica spin column (Epoch Life Sciences), rinsed twice with 750 μl of NW buffer (5 mM Tris-HCl [pH 7.5],

50 mM NaCl, 5 mM EDTA, 50% ethanol), and spun for 5 min at 2,000 $\times$ *g* to dry, and then polyP, DNA, and RNA were eluted in 150 μl of 50 mM Tris-HCl, pH 8. The eluate was brought to 20 mM Tris-HCl (pH 7.5), 5 mM MgCl$_2$, and 50 mM ammonium acetate in a final volume of 200 μl with 1 μg of the polyP-specific phosphatase PPX1 from *Saccharomyces cerevisiae* (111) and incubated for 15 min at 37°C. The resulting polyP-derived free phosphate was measured using a malachite green colorimetric assay (112) and normalized to total protein.

PolyP gel electrophoresis. PolyP-containing samples were separated on 10% or 15% acrylamide Tris-borate-EDTA (TBE)-urea gels (Bio-Rad) and negative stained with DAPI as previously described (67). PolyPs of defined lengths (averages of 14-, 60-, 130-, and 300-mers) were obtained from Toshikazu Shiba (RegenTiss, Inc.). For analysis of polyP accumulated *in vivo*, 1 ml of cells (A_{600} = 0.3 to 0.4) was pelleted by centrifugation, resuspended in 50 μl of GITC lysis buffer, and boiled for 10 min before 7.5 μl per lane was loaded with 2.5 μl of 6$\times$ DNA loading dye (Thermo Scientific).

Purification of PPK variants. Wild-type PPK was overexpressed with a C-terminal His$_6$ tag from plasmid pPPK2 and purified as previously described (14), using a nickel-charged 5-ml HiTrap chelating column and an ÅKTA Start fast-pressure liquid chromatography system (GE Healthcare Life Sciences). Variant proteins were overexpressed and purified from the pPPK2-derived plasmids pPPK14 through pPPK20 using the same protocol. Variants that overexpressed especially poorly (PPK^{N331D} and PPK^{M247I}) were further concentrated as previously described (113). Briefly, fractions containing PPK were pooled and dialyzed against 20 mM HEPES (pH 7.5), 15% glycerol, 1 mM EDTA, and 5 mM dithiothreitol (DTT) containing 0.2 M NaCl and then applied to a cation exchange column (1-ml HiTrap SP XL; GE Healthcare Life Sciences) and eluted with a linear salt gradient (0.2 to 0.8 M NaCl).

***In vitro* assays of PPK activity.** The specific activity for polyP synthesis of PPK wild-type and variant proteins was determined by a slight variation of a previously described method (56). Reaction mixtures (125-μl total volume) contained 5 nM PPK, 50 mM HEPES-KOH (pH 7.5), 50 mM ammonium sulfate, 5 mM MgCl$_2$, and, unless otherwise indicated, 20 mM creatine phosphate and 60 μg ml^{-1} of creatine kinase. Reaction mixtures were prewarmed to 37°C, and then reactions were started by addition of MgATP to a final concentration of 6 mM. For fluorescent detection of polyP (56), aliquots (20 μl) were removed from 125-μl reaction mixtures at 1, 2, 3, and 4 min and stopped by dilution into 80 μl of 62.5 mM EDTA–50 μM DAPI in black 96-well plates. Steady-state polyP-DAPI fluorescence (excitation wavelength, 415 nm; emission wavelength, 600 nm) was measured in an Infinite M1000 Pro microplate reader (Tecan Group, Ltd.). The polyP content of each sample (calculated in terms of individual phosphate monomers) was determined by comparison to a standard curve of commercially available polyP (Acros Organics) (0 to 150 μM), and rates of polyP synthesis were calculated by linear regression (Prism 7; GraphPad Software, Inc.).

For determination of kinetic constants, rates of polyP synthesis were determined in 100-μl reaction mixtures containing 5 nM PPK, 50 mM HEPES-KOH (pH 7.5), 50 mM ammonium sulfate, 5 mM MgCl$_2$, 12 concentrations of MgATP ranging from 0 to 6 mM, and 8 concentrations of MgADP ranging from 0 to 3 mM. Reactions were stopped after 3 min by addition of 100 μl of 100 mM EDTA–80 μM DAPI, and polyP content was determined by fluorescence as described above. The resulting plots of rate of polyP synthesis versus MgATP concentration at various MgADP concentrations were fit using the competitive inhibition model equations K_m (observed) = $K_m \times (1 + [I]/K_i)$ and $Y = V_{max} \times X/[K_m$ (observed) $+ X]$, where X is the substrate concentration, Y is the enzyme activity, and I is the inhibitor concentration (Prism 7; GraphPad Software, Inc.). The overall r^2 was greater than 0.96 for all sets of fitted curves.

Data availability. All strains, plasmids, and computer code generated in the course of this work are available from the authors upon request.

SUPPLEMENTAL MATERIAL

ACKNOWLEDGMENTS

REFERENCES

1. Rao NN, Gomez-Garcia MR, Kornberg A. 2009. Inorganic polyphosphate: essential for growth and survival. Annu Rev Biochem 78:605–647. https://doi.org/10.1146/annurev.biochem.77.083007.093039.
2. Kulaev IS, Vagabov VM, Kulakovskaya TV (ed). 2004. The biochemistry of inorganic polyphosphates. John Wiley & Sons, Ltd., Chichester, West Sussex, England.
3. Morrissey JH, Smith SA. 2015. Polyphosphate as modulator of hemostasis, thrombosis, and inflammation. J Thromb Haemost 13(Suppl 1):S92–S97. https://doi.org/10.1111/jth.12896.
4. Azevedo C, Saiardi A. 2014. Functions of inorganic polyphosphates in eukaryotic cells: a coat of many colours. Biochem Soc Trans 42:98–102. https://doi.org/10.1042/BST20130111.

5. Omelon S, Georgiou J, Henneman ZJ, Wise LM, Sukhu B, Hunt T, Wynnyckyj C, Holmyard D, Bielecki R, Grynpas MD. 2009. Control of vertebrate skeletal mineralization by polyphosphates. PLoS One 4:e5634. https://doi.org/10.1371/journal.pone.0005634.

6. Cremers CM, Knoefler D, Gates S, Martin N, Dahl JU, Lempart J, Xie L, Chapman MR, Galvan V, Southworth DR, Jakob U. 2016. Polyphosphate: a conserved modifier of amyloidogenic processes. Mol Cell 63:768–780. https://doi.org/10.1016/j.molcel.2016.07.016.

7. Stotz SC, Scott LO, Drummond-Main C, Avchalumov Y, Girotto F, Davidsen J, Gomez-Garcia MR, Rho JM, Pavlov EV, Colicos MA. 2014. Inorganic polyphosphate regulates neuronal excitability through modulation of voltage-gated channels. Mol Brain 7:42. https://doi.org/10.1186/1756-6606-7-42.

8. Ahn K, Kornberg A. 1990. Polyphosphate kinase from Escherichia coli. Purification and demonstration of a phosphoenzyme intermediate. J Biol Chem 265:11734–11739.

9. Akiyama M, Crooke E, Kornberg A. 1992. The polyphosphate kinase gene of Escherichia coli. Isolation and sequence of the ppk gene and membrane location of the protein. J Biol Chem 267:22556–22561.

10. Racki LR, Tocheva EI, Dieterle MG, Sullivan MC, Jensen GJ, Newman DK. 2017. Polyphosphate granule biogenesis is temporally and functionally tied to cell cycle exit during starvation in Pseudomonas aeruginosa. Proc Natl Acad Sci U S A 114:E2440–E2449. https://doi.org/10.1073/pnas.1615575114.

11. Boutte CC, Henry JT, Crosson S. 2012. ppGpp and polyphosphate modulate cell cycle progression in Caulobacter crescentus. J Bacteriol 194:28–35. https://doi.org/10.1128/JB.05932-11.

12. Nomura K, Kato J, Takiguchi N, Ohtake H, Kuroda A. 2004. Effects of inorganic polyphosphate on the proteolytic and DNA-binding activities of Lon in Escherichia coli. J Biol Chem 279:34406–34410. https://doi.org/10.1074/jbc.M404725200.

13. Albi T, Serrano A. 2016. Inorganic polyphosphate in the microbial world. Emerging roles for a multifaceted biopolymer. World J Microbiol Biotechnol 32:27. https://doi.org/10.1007/s11274-015-1983-2.

14. Gray MJ, Wholey W-Y, Wagner NO, Cremers CM, Mueller-Schickert A, Hock NT, Krieger AG, Smith EM, Bender RA, Bardwell JCA, Jakob U. 2014. Polyphosphate is a primordial chaperone. Mol Cell 53:689–699. https://doi.org/10.1016/j.molcel.2014.01.012.

15. Grillo-Puertas M, Schurig-Briccio LA, Rodriguez-Montelongo L, Rintoul MR, Rapisarda VA. 2014. Copper tolerance mediated by polyphosphate degradation and low-affinity inorganic phosphate transport system in Escherichia coli. BMC Microbiol 14:72. https://doi.org/10.1186/1471-2180-14-72.

16. Albi T, Serrano A. 2015. Two strictly polyphosphate-dependent gluco-(manno)kinases from diazotrophic cyanobacteria with potential to phosphorylate hexoses from polyphosphates. Appl Microbiol Biotechnol 99:3887–3900. https://doi.org/10.1007/s00253-014-6184-7.

17. Klemke F, Beyer G, Sawade L, Saitov A, Korte T, Maldener I, Lockau W, Nurnberg DJ, Volkmer T. 2014. All1371 is a polyphosphate-dependent glucokinase in Anabaena sp. PCC 7120. Microbiology 160:2807–2819.

18. Rashid MH, Kornberg A. 2000. Inorganic polyphosphate is needed for swimming, swarming, and twitching motilities of Pseudomonas aeruginosa. Proc Natl Acad Sci U S A 97:4885–4890. https://doi.org/10.1073/pnas.060030097.

19. Gray MJ, Jakob U. 2015. Oxidative stress protection by polyphosphate—new roles for an old player. Curr Opin Microbiol 24:1–6. https://doi.org/10.1016/j.mib.2014.12.004.

20. Peng YC, Lu C, Li G, Eichenbaum Z, Lu CD. 2017. Induction of the pho regulon and polyphosphate synthesis against spermine stress in Pseudomonas aeruginosa. Mol Microbiol 104:1037–1051. https://doi.org/10.1111/mmi.13678.

21. Amado L, Kuzminov A. 2009. Polyphosphate accumulation in Escherichia coli in response to defects in DNA metabolism. J Bacteriol 191:7410–7416. https://doi.org/10.1128/JB.01138-09.

22. Cha SB, Rayamajhi N, Lee WJ, Shin MK, Jung MH, Shin SW, Kim JW, Yoo HS. 2012. Generation and envelope protein analysis of internalization defective Brucella abortus mutants in professional phagocytes, RAW 2647. FEMS Immunol Med Microbiol 64:244–254. https://doi.org/10.1111/j.1574-695X.2011.00896.x.

23. Candon HL, Allan BJ, Fraley CD, Gaynor EC. 2007. Polyphosphate kinase 1 is a pathogenesis determinant in Campylobacter jejuni. J Bacteriol 189:8099–8108. https://doi.org/10.1128/JB.01037-07.

24. Richards MI, Michell SL, Oyston PC. 2008. An intracellularly inducible gene involved in virulence and polyphosphate production in Francisella. J Med Microbiol 57:1183–1192. https://doi.org/10.1099/jmm.0.2008/001826-0.

25. Ayraud S, Janvier B, Labigne A, Ecobichon C, Burucoa C, Fauchere JL. 2005. Polyphosphate kinase: a new colonization factor of Helicobacter pylori. FEMS Microbiol Lett 243:45–50. https://doi.org/10.1016/j.femsle.2004.11.040.

26. Singh R, Singh M, Arora G, Kumar S, Tiwari P, Kidwai S. 2013. Polyphosphate deficiency in Mycobacterium tuberculosis is associated with enhanced drug susceptibility and impaired growth in guinea pigs. J Bacteriol 195:2839–2851. https://doi.org/10.1128/JB.00038-13.

27. Rashid MH, Rumbaugh K, Passador L, Davies DG, Hamood AN, Iglewski BH, Kornberg A. 2000. Polyphosphate kinase is essential for biofilm development, quorum sensing, and virulence of Pseudomonas aeruginosa. Proc Natl Acad Sci U S A 97:9636–9641. https://doi.org/10.1073/pnas.170283397.

28. Kim KS, Rao NN, Fraley CD, Kornberg A. 2002. Inorganic polyphosphate is essential for long-term survival and virulence factors in Shigella and Salmonella spp. Proc Natl Acad Sci U S A 99:7675–7680. https://doi.org/10.1073/pnas.112210499.

29. Barnard JL, Dunlap P, Steichen M. 2017. Rethinking the mechanisms of biological phosphorus removal. Water Environ Res 89:2043–2054. https://doi.org/10.2175/106143017X15051465919010.

30. He S, McMahon KD. 2011. Microbiology of 'Candidatus Accumulibacter' in activated sludge. Microb Biotechnol 4:603–619. https://doi.org/10.1111/j.1751-7915.2011.00248.x.

31. McMahon KD, Yilmaz S, He S, Gall DL, Jenkins D, Keasling JD. 2007. Polyphosphate kinase genes from full-scale activated sludge plants. Appl Microbiol Biotechnol 77:167–173. https://doi.org/10.1007/s00253-007-1122-6.

32. Keasling JD, Van Dien SJ, Pramanik J. 1998. Engineering polyphosphate metabolism in Escherichia coli: implications for bioremediation of inorganic contaminants. Biotechnol Bioeng 58:231–239. https://doi.org/10.1002/(SICI)1097-0290(19980420)58:2/3<231::AID-BIT16>3.0.CO;2-F.

33. Kato J, Yamada K, Muramatsu A, Hardoyo Ohtake H. 1993. Genetic improvement of Escherichia coli for enhanced biological removal of phosphate from wastewater. Appl Environ Microbiol 59:3744–3749.

34. Jones KL, Kim SW, Keasling JD. 2000. Low-copy plasmids can perform as well as or better than high-copy plasmids for metabolic engineering of bacteria. Metab Eng 2:328–338. https://doi.org/10.1006/mben.2000.0161.

35. Liang M, Frank S, Lunsdorf H, Warren MJ, Prentice MB. 2017. Bacterial microcompartment-directed polyphosphate kinase promotes stable polyphosphate accumulation in E. coli. Biotechnol J 12:1600415. https://doi.org/10.1002/biot.201600415.

36. Ishige K, Zhang H, Kornberg A. 2002. Polyphosphate kinase (PPK2), a potent, polyphosphate-driven generator of GTP. Proc Natl Acad Sci U S A 99:16684–16688. https://doi.org/10.1073/pnas.262655299.

37. Akiyama M, Crooke E, Kornberg A. 1993. An exopolyphosphatase of Escherichia coli. The enzyme and its ppx gene in a polyphosphate operon. J Biol Chem 268:633–639.

38. Ault-Riché D, Fraley CD, Tzeng CM, Kornberg A. 1998. Novel assay reveals multiple pathways regulating stress-induced accumulations of inorganic polyphosphate in Escherichia coli. J Bacteriol 180:1841–1847.

39. Kuroda A, Murphy H, Cashel M, Kornberg A. 1997. Guanosine tetra- and pentaphosphate promote accumulation of inorganic polyphosphate in Escherichia coli. J Biol Chem 272:21240–21243. https://doi.org/10.1074/jbc.272.34.21240.

40. Gaca AO, Colomer-Winter C, Lemos JA. 2015. Many means to a common end: the intricacies of (p)ppGpp metabolism and its control of bacterial homeostasis. J Bacteriol 197:1146–1156. https://doi.org/10.1128/JB.02577-14.

41. Potrykus K, Cashel M. 2008. (p)ppGpp: still magical? Annu Rev Microbiol 62:35–51. https://doi.org/10.1146/annurev.micro.62.081307.162903.

42. Rao NN, Liu S, Kornberg A. 1998. Inorganic polyphosphate in Escherichia coli: the phosphate regulon and the stringent response. J Bacteriol 180:2186–2193.

43. Yang C, Huang TW, Wen SY, Chang CY, Tsai SF, Wu WF, Chang CH. 2012. Genome-wide PhoB binding and gene expression profiles reveal the hierarchical gene regulatory network of phosphate starvation in Escherichia coli. PLoS One 7:e47314. https://doi.org/10.1371/journal.pone.0047314.

44. Yuan ZC, Zaheer R, Morton R, Finan TM. 2006. Genome prediction of PhoB regulated promoters in Sinorhizobium meliloti and twelve pro-

teobacteria. Nucleic Acids Res 34:2686–2697. https://doi.org/10.1093/nar/gkl365.

45. Zimmer DP, Soupene E, Lee HL, Wendisch VF, Khodursky AB, Peter BJ, Bender RA, Kustu S. 2000. Nitrogen regulatory protein C-controlled genes of Escherichia coli: scavenging as a defense against nitrogen limitation. Proc Natl Acad Sci U S A 97:14674–14679. https://doi.org/10.1073/pnas.97.26.14674.

46. Maciag A, Peano C, Pietrelli A, Egli T, De Bellis G, Landini P. 2011. In vitro transcription profiling of the sigmaS subunit of bacterial RNA polymerase: re-definition of the sigmaS regulon and identification of sigmaS-specific promoter sequence elements. Nucleic Acids Res 39:5338–5355. https://doi.org/10.1093/nar/gkr129.

47. Durfee T, Hansen AM, Zhi H, Blattner FR, Jin DJ. 2008. Transcription profiling of the stringent response in Escherichia coli. J Bacteriol 190:1084–1096. https://doi.org/10.1128/JB.01092-07.

48. Wong GT, Bonocora RP, Schep AN, Beeler SM, Lee Fong AJ, Shull LM, Batachari LE, Dillon M, Evans C, Becker CJ, Bush EC, Hardin J, Wade JT, Stoebel DM. 23 January 2017. The genome-wide transcriptional response to varying RpoS levels in Escherichia coli K-12. J Bacteriol. https://doi.org/10.1128/JB.00755-16.

49. Patten CL, Kirchhof MG, Schertzberg MR, Morton RA, Schellhorn HE. 2004. Microarray analysis of RpoS-mediated gene expression in Escherichia coli K-12. Mol Genet Genomics 272:580–591. https://doi.org/10.1007/s00438-004-1089-2.

50. Weber H, Polen T, Heuveling J, Wendisch VF, Hengge R. 2005. Genome-wide analysis of the general stress response network in Escherichia coli: sigmaS-dependent genes, promoters, and sigma factor selectivity. J Bacteriol 187:1591–1603. https://doi.org/10.1128/JB.187.5.1591-1603.2005.

51. Dong T, Schellhorn HE. 2009. Control of RpoS in global gene expression of Escherichia coli in minimal media. Mol Genet Genomics 281:19–33. https://doi.org/10.1007/s00438-008-0389-3.

52. Dong T, Kirchhof MG, Schellhorn HE. 2008. RpoS regulation of gene expression during exponential growth of Escherichia coli K12. Mol Genet Genomics 279:267–277. https://doi.org/10.1007/s00438-007-0311-4.

53. Lacour S, Landini P. 2004. σ^S-Dependent gene expression at the onset of stationary phase in Escherichia coli: function of σ^S-dependent genes and identification of their promoter sequences. J Bacteriol 186:7186–7195. https://doi.org/10.1128/JB.186.21.7186-7195.2004.

54. Shiba T, Tsutsumi K, Yano H, Ihara Y, Kameda A, Tanaka K, Takahashi H, Munekata M, Rao NN, Kornberg A. 1997. Inorganic polyphosphate and the induction of rpoS expression. Proc Natl Acad Sci U S A 94:11210–11215. https://doi.org/10.1073/pnas.94.21.11210.

55. Kusano S, Ishihama A. 1997. Functional interaction of Escherichia coli RNA polymerase with inorganic polyphosphate. Genes Cells 2:433–441. https://doi.org/10.1046/j.1365-2443.1997.13203301320330.x.

56. Dahl JU, Gray MJ, Bazopoulou D, Beaufay F, Lempart J, Koenigsknecht MJ, Wang Y, Baker JR, Hasler WL, Young VB, Sun D, Jakob U. 2017. The anti-inflammatory drug mesalamine targets bacterial polyphosphate accumulation. Nat Microbiol 2:16267. https://doi.org/10.1038/nmicrobiol.2016.267.

57. Gardner SG, Johns KD, Tanner R, McCleary WR. 2014. The PhoU protein from Escherichia coli interacts with PhoR, PstB, and metals to form a phosphate-signaling complex at the membrane. J Bacteriol 196:1741–1752. https://doi.org/10.1128/JB.00029-14.

58. Morohoshi T, Maruo T, Shirai Y, Kato J, Ikeda T, Takiguchi N, Ohtake H, Kuroda A. 2002. Accumulation of inorganic polyphosphate in phoU mutants of Escherichia coli and Synechocystis sp. strain PCC6803. Appl Environ Microbiol 68:4107–4110. https://doi.org/10.1128/AEM.68.8.4107-4110.2002.

59. Hirota R, Motomura K, Nakai S, Handa T, Ikeda T, Kuroda A. 2013. Stable polyphosphate accumulation by a pseudo-revertant of an Escherichia coli phoU mutant. Biotechnol Lett 35:695–701. https://doi.org/10.1007/s10529-012-1133-y.

60. de Almeida LG, Ortiz JH, Schneider RP, Spira B. 2015. phoU inactivation in Pseudomonas aeruginosa enhances accumulation of ppGpp and polyphosphate. Appl Environ Microbiol 81:3006–3015. https://doi.org/10.1128/AEM.04168-14.

61. Kim HY, Schlictman D, Shankar S, Xie Z, Chakrabarty AM, Kornberg A. 1998. Alginate, inorganic polyphosphate, GTP and ppGpp synthesis co-regulated in Pseudomonas aeruginosa: implications for stationary phase survival and synthesis of RNA/DNA precursors. Mol Microbiol 27:717–725. https://doi.org/10.1046/j.1365-2958.1998.00702.x.

62. Sureka K, Dey S, Datta P, Singh AK, Dasgupta A, Rodrigue S, Basu J,

Kundu M. 2007. Polyphosphate kinase is involved in stress-induced mprAB-sigE-rel signalling in mycobacteria. Mol Microbiol 65:261–276. https://doi.org/10.1111/j.1365-2958.2007.05814.x.

63. Maisonneuve E, Castro-Camargo M, Gerdes K. 2013. (p)ppGpp controls bacterial persistence by stochastic induction of toxin-antitoxin activity. Cell 154:1140–1150. https://doi.org/10.1016/j.cell.2013.07.048.

64. Manganelli R. 2007. Polyphosphate and stress response in mycobacteria. Mol Microbiol 65:258–260. https://doi.org/10.1111/j.1365-2958.2007.05819.x.

65. Lee WD, Gawri R, Shiba T, Ji AR, Stanford WL, Kandel RA. 16 March 2017. Simple silica column-based method to quantify inorganic polyphosphates in cartilage and other tissues. Cartilage https://doi.org/10.1177/1947603517690856:1947603517690856.

66. Bru S, Jimenez J, Canadell D, Arino J, Clotet J. 2016. Improvement of biochemical methods of polyP quantification. Microb Cell 4:6–15. https://doi.org/10.1186/s40168-016-0152-7.

67. Smith SA, Morrissey JH. 2007. Sensitive fluorescence detection of polyphosphate in polyacrylamide gels using 4′,6-diamidino-2-phenylindol. Electrophoresis 28:3461–3465. https://doi.org/10.1002/elps.200700041.

68. Livermore TM, Chubb JR, Saiardi A. 2016. Developmental accumulation of inorganic polyphosphate affects germination and energetic metabolism in Dictyostelium discoideum. Proc Natl Acad Sci U S A 113:996–1001. https://doi.org/10.1073/pnas.1519440113.

69. Gray MJ, Wholey WY, Parker BW, Kim M, Jakob U. 2013. NemR is a bleach-sensing transcription factor. J Biol Chem 288:13789–13798. https://doi.org/10.1074/jbc.M113.454421.

70. Wang S, Deng K, Zaremba S, Deng X, Lin C, Wang Q, Tortorello ML, Zhang W. 2009. Transcriptomic response of Escherichia coli O157:H7 to oxidative stress. Appl Environ Microbiol 75:6110–6123. https://doi.org/10.1128/AEM.00914-09.

71. Chen J, Su L, Wang X, Zhang T, Liu F, Chen H, Tan C. 2016. Polyphosphate kinase mediates antibiotic tolerance in extraintestinal pathogenic Escherichia coli PCN033. Front Microbiol 7:724. https://doi.org/10.3389/fmicb.2016.00724.

72. Guzman LM, Belin D, Carson MJ, Beckwith J. 1995. Tight regulation, modulation, and high-level expression by vectors containing the arabinose PBAD promoter. J Bacteriol 177:4121–4130. https://doi.org/10.1128/jb.177.14.4121-4130.1995.

73. Curtis SJ, Epstein W. 1975. Phosphorylation of D-glucose in Escherichia coli mutants defective in glucosephosphotransferase, mannosephosphotransferase, and glucokinase. J Bacteriol 122:1189–1199.

74. Escalante A, Salinas Cervantes A, Gosset G, Bolivar F. 2012. Current knowledge of the Escherichia coli phosphoenolpyruvate-carbohydrate phosphotransferase system: peculiarities of regulation and impact on growth and product formation. Appl Microbiol Biotechnol 94:1483–1494. https://doi.org/10.1007/s00253-012-4101-5.

75. Luo Y, Zhang T, Wu H. 2014. The transport and mediation mechanisms of the common sugars in Escherichia coli. Biotechnol Adv 32:905–919. https://doi.org/10.1016/j.biotechadv.2014.04.009.

76. Datsenko KA, Wanner BL. 2000. One-step inactivation of chromosomal genes in Escherichia coli K-12 using PCR products. Proc Natl Acad Sci U S A 97:6640–6645. https://doi.org/10.1073/pnas.120163297.

77. Aguilar C, Escalante A, Flores N, de Anda R, Riveros-McKay F, Gosset G, Morett E, Bolivar F. 2012. Genetic changes during a laboratory adaptive evolution process that allowed fast growth in glucose to an Escherichia coli strain lacking the major glucose transport system. BMC Genomics 13:385. https://doi.org/10.1186/1471-2164-13-385.

78. Flores N, Xiao J, Berry A, Bolivar F, Valle F. 1996. Pathway engineering for the production of aromatic compounds in Escherichia coli. Nat Biotechnol 14:620–623.

79. Wang RF, Kushner SR. 1991. Construction of versatile low-copy-number vectors for cloning, sequencing and gene expression in Escherichia coli. Gene 100:195–199.

80. Rasila TS, Pajunen MI, Savilahti H. 2009. Critical evaluation of random mutagenesis by error-prone polymerase chain reaction protocols, Escherichia coli mutator strain, and hydroxylamine treatment. Anal Biochem 388:71–80. https://doi.org/10.1016/j.ab.2009.02.008.

81. Cini N, Ball V. 2014. Polyphosphates as inorganic polyelectrolytes interacting with oppositely charged ions, polymers and deposited on surfaces: fundamentals and applications. Adv Colloid Interface Sci 209:84–97. https://doi.org/10.1016/j.cis.2014.01.011.

82. Wacker WE. 1969. The biochemistry of magnesium. Ann N Y Acad Sci 162:717–726.

83. Christensen DG, Orr JS, Rao CV, Wolfe AJ. 2017. Increasing growth yield and decreasing acetylation in Escherichia coli by optimizing the carbon-to-magnesium ratio in peptide-based media. Appl Environ Microbiol 83:e03034-16. https://doi.org/10.1128/AEM.03034-16.

84. Aschar-Sobbi R, Abramov AY, Diao C, Kargacin ME, Kargacin GJ, French RJ, Pavlov E. 2008. High sensitivity, quantitative measurements of polyphosphate using a new DAPI-based approach. J Fluoresc 18: 859–866. https://doi.org/10.1007/s10895-008-0315-4.

85. Bennett BD, Kimball EH, Gao M, Osterhout R, Van Dien SJ, Rabinowitz JD. 2009. Absolute metabolite concentrations and implied enzyme active site occupancy in Escherichia coli. Nat Chem Biol 5:593–599. https://doi.org/10.1038/nchembio.186.

86. Zhu Y, Huang W, Lee SS, Xu W. 2005. Crystal structure of a polyphosphate kinase and its implications for polyphosphate synthesis. EMBO Rep 6:681–687. https://doi.org/10.1038/sj.embor.7400448.

87. Tzeng CM, Kornberg A. 2000. The multiple activities of polyphosphate kinase of Escherichia coli and their subunit structure determined by radiation target analysis. J Biol Chem 275:3977–3983. https://doi.org/10.1074/jbc.275.6.3977.

88. Emsley P, Lohkamp B, Scott WG, Cowtan K. 2010. Features and development of Coot. Acta Crystallogr D Biol Crystallogr 66:486–501. https://doi.org/10.1107/S0907444910007493.

89. Krissinel E, Henrick K. 2007. Inference of macromolecular assemblies from crystalline state. J Mol Biol 372:774–797. https://doi.org/10.1016/j.jmb.2007.05.022.

90. Kumble KD, Ahn K, Kornberg A. 1996. Phosphohistidyl active sites in polyphosphate kinase of Escherichia coli. Proc Natl Acad Sci U S A 93:14391–14395.

91. Amato SM, Orman MA, Brynildsen MP. 2013. Metabolic control of persister formation in Escherichia coli. Mol Cell 50:475–487. https://doi.org/10.1016/j.molcel.2013.04.002.

92. Kimura S, Makino K, Shinagawa H, Amemura M, Nakata A. 1989. Regulation of the phosphate regulon of Escherichia coli: characterization of the promoter of the pstS gene. Mol Gen Genet 215:374–380.

93. Schurig-Briccio LA, Farias RN, Rintoul MR, Rapisarda VA. 2009. Phosphate-enhanced stationary-phase fitness of Escherichia coli is related to inorganic polyphosphate level. J Bacteriol 191:4478–4481. https://doi.org/10.1128/JB.00082-09.

94. Munevar NF, de Almeida LG, Spira B. 2017. Differential regulation of polyphosphate genes in Pseudomonas aeruginosa. Mol Genet Genomics 292:105–116. https://doi.org/10.1007/s00438-016-1259-z.

95. Lindner SN, Knebel S, Wesseling H, Schoberth SM, Wendisch VF. 2009. Exopolyphosphatases PPX1 and PPX2 from Corynebacterium glutamicum. Appl Environ Microbiol 75:3161–3170. https://doi.org/10.1128/AEM.02705-08.

96. Albi T, Serrano A. 2014. Two exopolyphosphatases with distinct molecular architectures and substrate specificities from the thermophilic green-sulfur bacterium Chlorobium tepidum TLS. Microbiology 160: 2067–2078. https://doi.org/10.1099/mic.0.080952-0.

97. Wang X, Wang X, Hui K, Wei W, Zhang W, Miao A, Xiao L, Yang L. 30 November 2017. Highly effective polyphosphate synthesis, phosphate removal, and concentration using engineered environmental bacteria based on a simple solo medium-copy plasmid strategy. Environ Sci Technol https://doi.org/10.1021/acs.est.7b04532.

98. Sambrook J, Fritsch EF, Maniatis T. 1989. Molecular cloning: a laboratory manual, 2nd ed. Cold Spring Harbor Laboratory Press, Cold Spring Harbor, NY.

99. Bertani G. 1951. Studies on lysogenesis. I. The mode of phage liberation by lysogenic Escherichia coli. J Bacteriol 62:293–300.

100. Kuroda A, Tanaka S, Ikeda T, Kato J, Takiguchi N, Ohtake H. 1999. Inorganic polyphosphate kinase is required to stimulate protein degradation and for adaptation to amino acid starvation in Escherichia coli. Proc Natl Acad Sci U S A 96:14264–14269.

101. Chen IA, Markowitz VM, Chu K, Palaniappan K, Szeto E, Pillay M, Ratner A, Huang J, Andersen E, Huntemann M, Varghese N, Hadjithomas M, Tennessen K, Nielsen T, Ivanova NN, Kyrpides NC. 2017. IMG/M: integrated genome and metagenome comparative data analysis system. Nucleic Acids Res 45:D507–D516. https://doi.org/10.1093/nar/gkw929.

102. Cock PJ, Antao T, Chang JT, Chapman BA, Cox CJ, Dalke A, Friedberg I, Hamelryck T, Kauff F, Wilczynski B, de Hoon MJ. 2009. Biopython: freely available Python tools for computational molecular biology and bioinformatics. Bioinformatics 25:1422–1423. https://doi.org/10.1093/bioinformatics/btp163.

103. Edgar RC. 2004. MUSCLE: multiple sequence alignment with high accuracy and high throughput. Nucleic Acids Res 32:1792–1797. https://doi.org/10.1093/nar/gkh340.

104. Crooks GE, Hon G, Chandonia JM, Brenner SE. 2004. WebLogo: a sequence logo generator. Genome Res 14:1188–1190. https://doi.org/10.1101/gr.849004.

105. Silhavy TJ, Berman ML, Enquist LW (ed). 1984. Experiments with gene fusions. Cold Spring Harbor Laboratory, Cold Spring Harbor, NY.

106. Baba T, Ara T, Hasegawa M, Takai Y, Okumura Y, Baba M, Datsenko KA, Tomita M, Wanner BL, Mori H. 2006. Construction of Escherichia coli K-12 in-frame, single-gene knockout mutants: the Keio collection. Mol Syst Biol 2:2006.0008. https://doi.org/10.1038/msb4100050.

107. Blattner FR, Plunkett G, III, Bloch CA, Perna NT, Burland V, Riley M, Collado-Vides J, Glasner JD, Rode CK, Mayhew GF, Gregor J, Davis NW, Kirkpatrick HA, Goeden MA, Rose DJ, Mau B, Shao Y. 1997. The complete genome sequence of Escherichia coli K-12. Science 277: 1453–1462.

108. Studier FW, Rosenberg AH, Dunn JJ, Dubendorff JW. 1990. Use of T7 RNA-polymerase to direct expression of cloned genes. Methods Enzymol 185: 60–89.

109. Khan SR, Gaines J, Roop RM, II, Farrand SK. 2008. Broad-host-range expression vectors with tightly regulated promoters and their use to examine the influence of TraR and TraM expression on Ti plasmid quorum sensing. Appl Environ Microbiol 74:5053–5062. https://doi.org/10.1128/AEM.01098-08.

110. Wilson KJ, Hughes SG, Jefferson RA. 1992. The Escherichia coli gus operon: induction and expression of the gus operon in E. coli and the occurrence and use of GUS in other bacteria, p 7–22. In Gallagher SR (ed), GUS protocols using the GUS gene as a reporter of gene expression. Academic Press, Inc, San Diego, CA.

111. Wurst H, Kornberg A. 1994. A soluble exopolyphosphatase of Saccharomyces cerevisiae. Purification and characterization. J Biol Chem 269: 10996–11001.

112. Carter SG, Karl DW. 1982. Inorganic phosphate assay with malachite green: an improvement and evaluation. J Biochem Biophys Methods 7:7–13.

113. Zhu Y, Lee SS, Xu W. 2003. Crystallization and characterization of polyphosphate kinase from Escherichia coli. Biochem Biophys Res Commun 305:997–1001. https://doi.org/10.1016/S0006-291X(03)00886-6.